Networks and Heterogeneous Media

https://www.aimspress.com/journal/nhm

NHM, 21(4): 1334–1375.
DOI: 10.3934/nhm.2026051
Received: 19 March 2026
Revised: 13 June 2026
Accepted: 26 June 2026
Published: 03 July 2026

Research article

Dynamics and optimal control of a fractional-order propagation model with time-varying intervention costs

Li Wang and Zongmin Yue*

School of Mathematics and Data Science, Shaanxi University of Science and Technology, Xi'an 710021, China

* **Correspondence:** Email: joanna_yzm@163.com.

Abstract: The growing role of artificial intelligence (AI) in information dissemination has made algorithmic recommendation a significant pathway for rumor spread. To address this, we developed a dual-path rumor propagation model that integrates interpersonal communication with AI-driven algorithmic diffusion. The model employs Caputo fractional derivatives to capture memory effects and historical dependencies in the spreading process. For intervention, we proposed a coordinated control framework combining traditional measures (e.g., legal regulation and science education) with dynamic AI algorithmic control. A key innovation was the design of a time-varying cost function and the introduction of a time-sensitive factor to model the realistic constraint of rising AI control costs over time, forming a novel fractional-order optimal control problem. The trade-off between control cost and governance effectiveness was analyzed via Pareto frontier optimization. Theoretical analysis confirmed that the equilibrium and its global stability are governed by the basic reproduction number. Numerical simulations revealed the existence of a critical regime for the time-sensitive factor ($\rho = 0.8$), in which the optimal strategy exhibits a distinct staged control behavior: intensive AI-based intervention is emphasized during the early phase, followed by a gradual transition toward traditional measures for sustained long-term governance. This strategy effectively reduces the peak and overall scale of rumor propagation, demonstrates robustness across parameters, and achieves a balanced trade-off between control cost and social benefit. The study provides a dynamic modeling framework for rumor governance in the AI era, highlighting the importance of integrating algorithmic and traditional controls while accounting for time-varying costs.

Keywords: fractional-order optimal control; time-varying cost; time-sensitive factor; Pareto frontier; rumor propagation control

1. Introduction

Driven by algorithms, we are entering an era of artificial intelligence “ghostwriting”: Large language models can draft emails, generate reports, and even produce “scientific discourse” convincing enough to blur the lines between truth and falsehood. For instance, reference [1] demonstrated that large language models can generate high-quality multilingual content via mixture-of-experts techniques, further lowering the barrier for producing convincing misinformation at scale. However, an increasingly acute contradiction has emerged from this—the fundamental conflict between humans’ growing trust in AI-generated content and the inherent uncertainty, biases, and even fallacies potentially embedded within such content. This conflict is particularly perilous in the realm of scientific communication. When an unverified “groundbreaking study” is rapidly disseminated by AI systems in a professional and credible textual format, it ceases to be mere informational noise and may evolve into a cognitive epidemic cloaked in the guise of science. AI-driven rumors, characterized by their efficiency, realism, and capacity for large-scale personalization, are reshaping the ecology of rumor propagation. They are no longer slowly spreading misinformation but represent systemic cognitive risks delivered through “precision feeding.” This algorithm-dominated dissemination mode is transforming traditional social network structures into a complex ecosystem characterized by “deep human-algorithm coupling”, thereby amplifying the social harm of rumors. Uncontrolled AI rumor propagation not only disrupts normal online order but may also induce collective risks in the physical society. For instance, in 2023, an AI-generated rumor about “the bankruptcy of a certain bank” on a social platform, boosted by recommendation algorithms, quickly triggered regional financial contagion risk [2]. In the same year, a deepfake video synthesizing a “chemical plant explosion in a certain city” led to widespread social panic after being promoted through algorithmic recommendations [3]. These cases demonstrate that AI technology has become a key variable influencing the dynamics of rumor propagation.

The academic community has been closely examining the mechanisms through which algorithms influence information dissemination. Early studies often relied on classic infectious disease models, simplifying algorithmic impact into fixed transmission probability parameters [4–6]. As research progressed, scholars began treating recommendation algorithms as independent external driving forces, proposing improved models based on small-world and scale-free network theories [7, 8]. In recent years, some studies have attempted to endogenize algorithmic mechanisms, such as using time-varying parameters to characterize their adaptive features [9] or employing multi-layer network structures to describe the interaction between algorithms and users [10]. However, most of these models are based on integer-order differential equation frameworks, making it challenging to accurately capture the inherent memory effects and long-range dependency characteristics of algorithmic recommendation systems.

The core characteristic of AI recommendation systems lies in their dependency on historical data. User behaviors such as clicks, dwell time, and interactions are recorded by algorithms and utilized to optimize subsequent recommendations. This feedback mechanism based on historical behavior causes the rumor propagation process to exhibit significant memory effects. Leveraging the non-local operator properties of fractional calculus, its memory kernel function can effectively describe such long-range temporal correlations, providing a suitable mathematical tool for modeling rumor dissemination in AI-driven environments [11–13].

Traditional integer-order models assume that propagation dynamics depend only on current states, implicitly satisfying the Markov property and neglecting historical influences. However, AI-assisted recommendation platforms exhibit significant historical dependence and cumulative reinforcement effects. Recommendation algorithms continuously learn from users' previous interaction records, including browsing history, click behaviors, viewing duration, and repost frequency. Consequently, users previously exposed to rumor-related content remain more likely to encounter similar misinformation in the future due to persistent algorithmic reinforcement. For example, recommendation systems on TikTok, YouTube, and X (formerly Twitter) continuously analyze users' historical behaviors to generate personalized content streams. Even after users stop actively searching for rumor-related information, previously accumulated interaction histories may still trigger repeated recommendations of similar misinformation. This introduces long-range temporal dependence and persistent memory effects into the rumor-spreading process. In reality, AI-generated misinformation often exhibits delayed attenuation, repeated exposure, and secondary amplification-phenomena that classical memoryless integer-order equations cannot adequately capture. To characterize these nonlocal historical effects, this study adopts the Caputo fractional derivative, whose nonlocal memory kernel incorporates the cumulative influence of all previous states [14–16]. Thus, the current spreading rate depends not only on the present state but also on the entire historical propagation trajectory. The fractional order α quantifies memory persistence: As $\alpha \to 1$, the system degenerates to the classical integer-order model with weak historical dependence; smaller α indicates stronger memory effects and slower decay of algorithmic influence, meaning past rumor exposure continues to affect future propagation over longer time scales. This framework provides a more realistic mathematical description for AI-assisted rumor-spreading in modern intelligent recommendation environments.

In recent years, the Caputo-type fractional derivative has been widely applied in fields such as social network analysis [17] and recommendation algorithm optimization [18]. Regarding propagation modeling, existing research has developed various improved models, including the Susceptible-Infected-Recovered-Antagonistic (SIR-A) model that accounts for group polarization [19] and Susceptible-Exposed-Infected-Recovered (SEIR) models incorporating emotional factors [20]. Notably, Zhang et al. [21] were the first to introduce algorithm recommendation intensity as a state variable into a fractional-order model, offering an important reference for studying information dynamics in AI-influenced environments.

In the context of governance strategies, traditional approaches such as manual content review and rumor refutation are increasingly inadequate in coping with the high-speed propagation characteristics driven by algorithms. For complex network propagation dynamics, reference [22] established a theoretical and empirical framework for infectious disease control, providing methodological precedents for optimal intervention in networked spreading processes. Fractional-order optimal control theory offers a novel paradigm for designing adaptive intervention strategies [23–25]. By explicitly incorporating memory effects, this framework accounts for both the current dissemination state and the historical impact of interventions, thereby enabling more forward-looking control formulations. Recent advances have further extended fractional-order controllability theory to complex stochastic and delay systems [26, 27], providing mathematical foundations for rumor propagation models that involve random perturbations or delayed information feedback. In recent years, related methodologies have been applied to social network governance, giving rise to dynamic throttling algorithms [28] and adaptive clarification strategies [29]. Although these studies have achieved notable progress in rumor suppression, most existing models are constructed under the assumption of constant marginal control costs [30, 31]. However, in practical algorithmic governance scenarios, control costs often exhibit pronounced time sensitivity. Prolonged algorithmic restrictions or high-intensity content filtering may gradually degrade user experience and reduce platform activity, generating opportunity costs that accumulate in a nonlinear manner over time [32]. Motivated by these considerations, it becomes necessary to introduce time-varying cost functions—particularly those capturing temporal discounting effects [33]—into the optimal control framework. Such formulations provide a more realistic foundation for analyzing how different governance measures should be allocated over time under real-world constraints.

Compared with existing rumor propagation and optimal control models, the proposed framework integrates AI-driven dissemination dynamics, fractional-order memory effects, and time-varying intervention costs within a unified modeling and control framework.

Building upon existing research, this paper advances the modeling and control of AI-driven rumor propagation in three key dimensions. First, at the modeling level, we incorporate "AI transmission activity" as an independent, dynamic state variable within a fractional-order system. Utilizing the memory properties of fractional calculus, this approach quantifies how recommendation algorithms rely on historical data to drive rumor diffusion, rather than treating them as static parameters. Second, at the control theory level, we formulated a fractional-order optimal control problem with time-varying costs. By introducing a temporal cost function, we identify a time-dependent governance strategy, in which algorithmic interventions are emphasized during periods of rapid information amplification, while sustained social governance measures are gradually strengthened to support long-term regulation.

Finally, at the governance strategy level, simulations illustrate a stage-based hierarchical control framework: applying intensive technical regulation in the early stage to limit rapid rumor amplification, reinforcing legal accountability in the intermediate stage to maintain regulatory effectiveness, and strengthening public education in the later stage to consolidate long-term stability. This framework provides a theoretical foundation for the integrated application of technical and social governance measures.

The structure of this paper is organized as follows: Section 2 introduces the fundamental theory of fractional calculus, Section 3 constructs a fractional-order rumor propagation model incorporating AI transmission activity, Section 4 analyzes the equilibrium points and stability of the model, Section 5 formulates and solves the fractional-order optimal control problem, Section 6 presents numerical simulations for validation, and Section 7 summarizes the paper and outlines future research directions.

2. Basic mathematical properties

The Caputo fractional derivative possesses an important nonlocal property: The system's current evolution depends on all historical states, not only instantaneous variables. Its memory kernel assigns weights to historical states based on temporal distance—recent behaviors exert stronger influence, while distant behaviors decay gradually but never vanish completely. This power-law memory structure aligns closely with the operating mechanism of modern AI recommendation systems. On AI-assisted platforms, recommendation algorithms continuously update user preference profiles based on accumulated interaction histories. Consequently, rumor dissemination exhibits persistent reinforcement: previously popular misinformation may continue to receive algorithmic exposure even after its immediate popularity declines. Thus, the propagation dynamics are inherently nonlocal and history-dependent, and the Caputo fractional derivative naturally captures this cumulative historical influence, providing a suitable mathematical framework for modeling persistent AI-driven rumor amplification.

Definition 1. *(Caputo fractional derivative [34, 35]).*

Let α be a positive real number ($\alpha > 0$), and $n - 1 \leq \alpha < n$, $n \in \mathbb{N}$. For a function $f(t)$ defined on the closed interval $[a, b]$, the α-order Caputo fractional derivative is defined as:

$$D^{\alpha} f(t) = \frac{1}{\Gamma(n-\alpha)} \int_a^t (t-\tau)^{n-\alpha-1} f^{(n)}(\tau)\, d\tau,$$

where $t \in [a, b]$, $\Gamma(\cdot)$ is the gamma function defined by $\Gamma(s) = \int_0^{\infty} t^{s-1} e^{-t}\, dt$.

3. Establishment of the model

In modern intelligent social media, rumor dissemination is no longer dominated solely by direct interpersonal interactions. AI-assisted recommendation algorithms reshape spreading dynamics through continuous feedback learning: once users interact with misinformation, the system records these behaviors and increases the probability of future exposure to similar content. Thus, current propagation intensity depends on both the present state and accumulated interaction histories. This persistent reinforcement introduces hereditary characteristics and long-range temporal dependence into rumor propagation. Classical integer-order equations assume instantaneous state transitions without memory accumulation, failing to capture the delayed attenuation and repeated exposure frequently observed in online rumor spreading. To incorporate these nonlocal historical effects, this study introduces the Caputo fractional derivative into the rumor propagation framework, enabling the model to characterize both current spreading behaviors and cumulative historical influences simultaneously.

To formulate the proposed AI-assisted rumor propagation model, the following assumptions are considered.

(1) Individuals repeatedly exposed to misinformation may gradually become rumor propagators due to cumulative psychological influence.

(2) AI recommendation systems continuously reinforce rumor dissemination according to users' historical interaction behaviors, including browsing records, click frequencies, and content engagement patterns.

(3) Historical recommendation accumulation introduces memory-dependent spreading characteristics into the dissemination process.

(4) The population is divided into different compartments according to their dissemination states, and the transition dynamics between these compartments are governed by the interaction mechanisms shown in the system in Eq (3.1).

Based on these assumptions, a fractional-order rumor propagation system in Eq (3.1) was established. The basic population information is as follows:

(1) Ignoramus ($I(t)$): Social-network users who have not yet been exposed to the rumor topic and remain unaware of related information. This group serves as potential recipients of the rumor.

Through algorithmic recommendations or social interactions with active users, they are highly susceptible to receiving information and undergoing state transition, acting as the “fuel” population for rumor diffusion.

(2) Latent user ($L(t)$): Users who have been exposed to the rumor or related information but have not yet taken substantive dissemination actions such as sharing or commenting. This group is in a phase of “information evaluation”. Due to information uncertainty or personal social conformity tendencies, they maintain a temporary wait-and-see attitude.

(3) Spreader ($S(t)$): Users who believe the rumor content and actively engage in forwarding, posting, liking, or inflammatory commenting online. Spreaders not only infect ignoramuses through social networks but also contribute to the algorithmic recognition of topic popularity. Their activity is captured by recommendation algorithms, thereby amplifying the AI-driven visibility of the topic and forming a “human-machine resonance” effect in dissemination.

(4) Clarifier ($C(t)$): Users who possess accurate information or critical thinking skills and proactively publish refutations, expose logical flaws in rumors, or counteract misinformation.

(5) Recovered ($R(t)$): Users who have completely ceased dissemination behavior due to loss of interest in the topic, shift in attention, or awareness of the truth but choose not to participate further in discussions.

(6) AI transmission activity ($A(t)$): A non-demographic macroscopic variable quantifying the degree of traffic amplification provided by algorithmic recommendation mechanisms on social-media platforms to rumor topics. This variable is stimulated by the activity of human spreaders and exhibits nonlinear growth through the self-reinforcing logic of algorithms. The specific model is as follows:

$$\begin{cases} D^{\alpha}I(t) = \varepsilon - \alpha IS - \theta_1 IC - \kappa AI - (\mu + d)I, \\ D^{\alpha}L(t) = \alpha IS + \theta_1 IC + \kappa AI - (\beta + \tau + \sigma + d)L, \\ D^{\alpha}S(t) = \beta L - \theta_2 SC - (\gamma + d)S, \\ D^{\alpha}C(t) = \tau L + \theta_2 SC - (\delta + d)C, \\ D^{\alpha}A(t) = \xi S + \phi\rho AI - \zeta A, \\ D^{\alpha}R(t) = \mu I + \sigma L + \gamma S + \delta C - dR. \end{cases} \tag{3.1}$$

The model diagram is as follows:

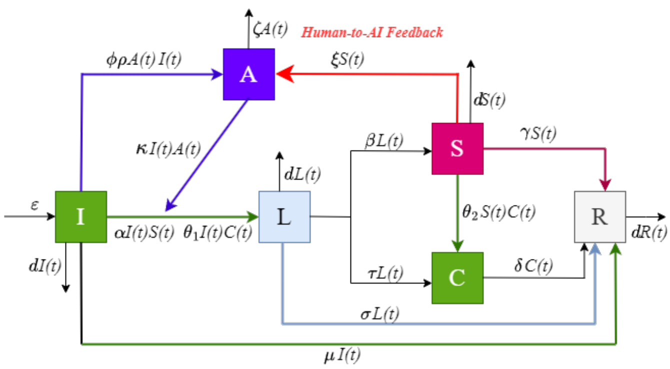

Figure 1. Basic framework diagram of the fractional-order human-AI rumor propagation model.

Figure 1 illustrates the interaction mechanism between human rumor-spreaders and AI-assisted recommendation systems. Historical user interaction behaviors continuously influence algorithmic recommendation probabilities, which in turn reinforce repeated misinformation exposure and further stimulate rumor dissemination.

(1) Input and Output Parameters

ε : Represents the number of new users entering the social network platform per unit of time. d: The rate at which users are removed from the system due to account cancellation, prolonged inactivity, or permanent departure from the platform. μ : The proportion of ignorant users (I) who transition directly to the recovered state (R) due to high media literacy or a complete lack of interest in the topic.

(2) Transmission and Conversion Parameters

α: The probability that an ignorant user (I) becomes interested in the rumor and converts into a latent user (L) after contact with a spreader (S). β : The probability that a latent user (L), after a period of psychological hesitation, chooses to believe and propagate the rumor, thereby becoming a spreader (S). τ: The probability that a latent user (L) identifies the fallacies within the rumor after evaluation and joins the debunking effort as a clarifier (C). σ : The rate at which latent users (L) find the information irrelevant and transition directly to the recovered state (R) without spreading or debunking the rumor.

(3) Confrontation and Recovery Parameters θ_1 : The rate at which ignorant users (I) transition to the latent state (L) upon exposure to information from clarifiers (C). θ_2 : A critical parameter measuring counter-rumor effectiveness; it represents the probability that a spreader (S) is persuaded by a clarifier (C) to stop spreading and become a clarifier. γ: The rate at which spreaders (S) naturally cease propagation and become recovered users (R) due to fading popularity or shifted attention. δ : The rate at which clarification activities naturally conclude.

(4) AI Dynamics Parameters κ : The rate at which ignorant users (I) are stimulated by high-frequency algorithmic recommendations (A) and transition into the latent state (L). ξ : The efficiency with which the active behavior of human spreaders (S) is captured by the system algorithm to increase AI topic popularity. ζ : The rate at which topic popularity naturally cools or AI recommendation intensity decreases due to platform regulation. ϕ : The coefficient representing the gain in system feedback driven by the algorithm. ρ : The probability of interaction between human users and the AI-driven system.

The corresponding initial conditions for the system in the Eq (3.1) are given by

$$I(0) = I_0, \quad L(0) = L_0, \quad S(0) = S_0, \quad C(0) = C_0, \quad A(0) = A_0, \quad R(0) = R_0,$$

where all initial values are assumed to be nonnegative.

In the formula, $I(t), L(t), S(t), C(t), R(t), A(t)$ represent the quantity of I, L, S, C, R, A at time t, respectively. $I(0), L(0), S(0), C(0), R(0), A(0) \geq 0$. $\varepsilon, d, \alpha, \kappa, \beta, \rho, \tau, \varphi, \delta, \theta_1, \theta_2, \gamma, \sigma, \xi, \zeta \in (0, 1)$. The specific parameter values can be found in Table 1. $N(t)$ represents the overall rumor dissemination system at time t. The numbers of ignorant individuals, latent individuals, disseminators, clarifiers, and suppressors at time t are respectively denoted as $I(t), L(t), S(t), C(t), R(t)$ and $A(t)$. Then we have

$$N(t) = I(t) + L(t) + S(t) + C(t) + A(t) + R(t). \tag{3.2}$$

Table 1. The meanings of each parameter value.

Parameters	Meaning
ε	External inflow rate
α	The contact rate of those who are ignorant and come into contact with the spreaders to those who become latent cases
θ_1	The rate at which the ignorant are influenced by clarification and transformed into latent individuals
κ	The influence rate of AI dissemination in turning ignorant individuals into latent ones
μ	The conversion rate of the ignorant to the rehabilitated individuals
d	The natural departure rates of various groups of people
β	The conversion rate from the latent group to the spreading group
τ	The conversion rate from lurkers to clarifiers
σ	The conversion rate of the latent individuals to the restorative ones
γ	The conversion rate of the communicator to the restorer
ϕ	The "amplification factor" or "recommendation enhancement coefficient" of the platform algorithm for click behaviors
ρ	The basic contribution rate of click actions
δ	The conversion rate from clarifiers to restorers
ξ	The intensity with which AI activity is influenced by the disseminator
ζ	The natural decay rate of the popularity of AI
θ_2	The rate at which the disseminators are persuaded to become clarifiers

Theorem 1. *The positive invariant set of the rumor propagation model of order β under the Caputo definition of order α in the model in Eq* (3.1) *is*

$$\Phi = \left\{(I(t), L(t), S(t), C(t), A(t), R(t)) \in \mathbb{R}_+^6 : I + L + S + C + R \leq \frac{\varepsilon}{d}, A \leq \frac{\varepsilon\xi}{d\left(\zeta - \varphi\rho\frac{\varepsilon}{d}\right)}\right\}. \tag{3.3}$$

Proof. Taking the Caputo fractional derivative of both sides of the model in Eq (3.1) and substituting it into the right-hand sides of the five equations of the model yields:

$$\begin{aligned}
D^\alpha N(t) &= D^\alpha I(t) + D^\alpha L(t) + D^\alpha S(t) + D^\alpha C(t) + D^\alpha R(t) \\
&= [\varepsilon - \alpha IS - \theta_1 IC - \kappa AI - (\mu + d)I] \\
&\quad + [\alpha IS + \theta_1 IC + \kappa AI - (\beta + \tau + \sigma + d)L] \\
&\quad + [\beta L - \theta_2 SC - (\gamma + d)S] + [\tau L + \theta_2 SC - (\delta + d)C] \\
&\quad + [\mu I + \sigma L + \gamma S + \delta C - dR] \\
&= \varepsilon - d(I + L + S + C + R) \\
&= \varepsilon - dN(t).
\end{aligned} \tag{3.4}$$

Equation (3.4) represents a linear fractional-order differential inequality, and its solution satisfies:

$$N(t) \leq \max\left\{N(0), \frac{\varepsilon}{d}\right\}.$$

In particular, if $N(0) \leq \frac{\varepsilon}{d}$, then $N(t) \leq \frac{\varepsilon}{d}$ holds true for all $t \geq 0$. Then the invariant set of the model in Eq (3.1) is

$$\Phi = \left\{ (I(t), L(t), S(t), C(t), A(t), R(t)) \in R_6^+ : I + L + S + C + R \leq \frac{\varepsilon}{d}, A \leq \frac{\varepsilon\xi}{d\left(\zeta - \phi\rho\frac{\varepsilon}{d}\right)} \right\}.$$

Theorem 2. *For any given initial condition $X(0) = (I_0, L_0, S_0, C_0, A_0, R_0)$, $\forall t \geq 0$, the model in Eq (3.1) has a unique solution $X(t) \in \Omega$.*

Proof. The existence and uniqueness of the solution are verified by using the method in reference [36].

Let $H(X) = (H_1(X), H_2(X), H_3(X), H_4(X), H_5(X), H_6(X))$:

$$\begin{aligned}
H_1(X) &= \varepsilon - \alpha IS - \theta_1 IC - \kappa AI - (\mu + d)I, \\
H_2(X) &= \alpha IS + \theta_1 IC + \kappa AI - (\beta + \tau + \sigma + d)L, \\
H_3(X) &= \beta L - \theta_2 SC - (\gamma + d)S, \\
H_4(X) &= \tau L + \theta_2 SC - (\delta + d)C, \\
H_5(X) &= \xi S + \phi\rho AI - \zeta A, \\
H_6(X) &= \mu I + \sigma L + \gamma S + \delta C - dR.
\end{aligned}$$

Furthermore, for any given $X, X_1 \in \Phi$, the following function can be constructed:

$$\begin{aligned}
\|H(X) - H(X_1)\| &= |H_1(X) - H_1(X_1)| + |H_2(X) - H_2(X_1)| + |H_3(X) - H_3(X_1)| \\
&\quad + |H_4(X) - H_4(X_1)| + |H_5(X) - H_5(X_1)| + |H_6(X) - H_6(X_1)| \\
&= |\varepsilon - \varepsilon| + |\alpha IS - \alpha I_1 S_1| + |\theta_1 IC - \theta_1 I_1 C_1| \\
&\quad + |\kappa AI - \kappa A_1 I_1| + |(\mu + d)(I - I_1)| \\
&\quad + |\alpha IS - \alpha I_1 S_1| + |\theta_1 IC - \theta_1 I_1 C_1| + |\kappa AI - \kappa A_1 I_1| \\
&\quad + |(\beta + \tau + \sigma + d)(L - L_1)| \\
&\quad + |\beta(L - L_1)| + |\theta_2(SC - S_1 C_1)| + |(\gamma + d)(S - S_1)| \\
&\quad + |\xi(S - S_1)| + |\phi\rho(AI - A_1 I_1)| + |\zeta(A - A_1)| \\
&\quad + |\mu(I - I_1)| + |\sigma(L - L_1)| + |\gamma(S - S_1)| \\
&\quad + |\delta(C - C_1)| + |d(R - R_1)| \\
&\leq l_1|I - I_1| + l_2|L - L_1| + l_3|S - S_1| + l_4|C - C_1| + l_5|A - A_1| + l_6|R - R_1| \\
&\leq L\|(I, L, S, C, A, R) - (I_1, L_1, S_1, C_1, A_1, R_1)\| \\
&\leq L\|X - X_1\|.
\end{aligned}$$

Among them,

$$l_1 = \frac{\varepsilon}{d}(\alpha + \theta_1 + \kappa) + \mu + d, \quad l_2 = \beta + \tau + \sigma + d, \quad l_3 = \theta_2\frac{\varepsilon}{d} + \gamma + d,$$
$$l_4 = \theta_2\frac{\varepsilon}{d} + \delta + d, \quad l_5 = \phi\rho\frac{\varepsilon}{d} + \zeta, \quad l_6 = d,$$

$$L = \max(l_1, l_2, l_3, l_4, l_5, l_6).$$

Therefore, for any initial condition $H(X)$ that satisfies the Lipschitz condition and $X(0) = (I_0, L_0, S_0, C_0, A_0, R_0)$, $\forall t \geq 0$, the model in Eq (3.1) always has a unique solution.

$R(t)$ has no effect on the first five equations in the model. This allows for dimensionality reduction of the system and the elimination of the state nodes of $R(t)$ in the differential equations. The simplified model is as follows:

$$\begin{cases} D^\alpha I(t) = \varepsilon - \alpha IS - \theta_1 IC - \kappa AI - (\mu + d)I, \\ D^\alpha L(t) = \alpha IS + \theta_1 IC + \kappa AI - (\beta + \tau + \sigma + d)L, \\ D^\alpha S(t) = \beta L - \theta_2 SC - (\gamma + d)S, \\ D^\alpha C(t) = \tau L + \theta_2 SC - (\delta + d)C, \\ D^\alpha A(t) = \xi S + \phi\rho AI - \zeta A. \end{cases} \tag{3.5}$$

4. Equilibrium and stability analysis of the model

This part calculates the equilibrium points and the basic reproduction number of the fractional-order network rumor propagation model, and uses the Lyapunov stability theorem [37] and the Routh-Hurwitz criterion [38] to discuss the stability of the equilibrium state of network rumor propagation. This section focuses on the local and global stability of the two equilibrium points, namely, point $RFEP(E_0)$ and the positive equilibrium point E^*.

4.1. No rumor equilibrium point and basic reproduction number

The rumor-free equilibrium (RFE) of the model in Eq (3.5) is denoted by $E_0 = (I_0, L_0, S_0, C_0, A_0)$, a state where the system contains neither rumor-spreaders, latent users, nor rumor-clarifiers. By setting the right-hand sides of the equations in the model in Eq (3.5) to zero, the system of equations is expressed as follows:

$$\begin{cases} \varepsilon - \alpha IS - \theta_1 IC - \kappa AI - (\mu + d)I = 0, \\ \alpha IS + \theta_1 IC + \kappa AI - (\beta + \tau + \sigma + d)L = 0, \\ \beta L - \theta_2 SC - (\gamma + d)S = 0, \\ \tau L + \theta_2 SC - (\delta + d)C = 0, \\ \xi S + \phi\rho AI - \zeta A = 0. \end{cases} \tag{4.1}$$

Next, we employ the concept of the basic reproduction number (R_0) [39] from classical epidemic modeling as a critical parameter to determine whether the rumor can be suppressed. Subsequent stability analysis is based on R_0. According to the definition, the unique equilibrium point is:

$$E_0 = (I_0, L_0, S_0, C_0, A_0) = \left(\frac{\varepsilon}{\mu + d}, 0, 0, 0, 0 \right).$$

The next-generation matrix method [40] is employed to solve for R_0, which is referred to as the spectral radius of the next-generation matrix.

Let $X(t) = (I(t), L(t), S(t), C(t), A(t))^T$, and then the model in Eq (3.5) can be written as:

$$D^{\alpha}X(t) = \Phi(x) - \Psi(x),$$

where

$$\Phi = \begin{bmatrix} \alpha IS + \theta_1 IC + \kappa IA \\ 0 \\ 0 \\ 0 \end{bmatrix}, \quad \Psi = \begin{bmatrix} (\beta + \tau + \sigma + d)L \\ -\beta L + (\gamma + d)S + \theta_2 SC \\ -\tau L + (\delta + d)C - \theta_2 SC \\ -\xi S + (\zeta - \phi\rho I_0)A \end{bmatrix}.$$

The Jacobian matrices for $\Phi(x)$ and $\Psi(x)$ at E_0 are calculated as follows:

$$f_0 = J(\Phi|E_0) = \begin{bmatrix} 0 & \alpha I_0 & \theta_1 I_0 & \kappa I_0 \\ 0 & 0 & 0 & 0 \\ 0 & 0 & 0 & 0 \\ 0 & 0 & 0 & 0 \end{bmatrix},$$

$$v_0 = J(\Psi|E_0) = \begin{bmatrix} \beta + \tau + \sigma + d & 0 & 0 & 0 \\ -\beta & \gamma + d & 0 & 0 \\ -\tau & 0 & \delta + d & 0 \\ 0 & -\xi & 0 & \zeta - \phi\rho I_0 \end{bmatrix}.$$

The next-generation matrix $f_0 v_0^{-1}$ is then computed:

$$f_0 v_0^{-1} = \begin{bmatrix} \frac{\alpha\beta I_0}{m(\gamma+d)} + \frac{\theta_1 \tau I_0}{m(\delta+d)} + \frac{\kappa\xi I_0}{m(\gamma+d)(\zeta-\phi\rho I_0)} & * & \frac{\theta_1 I_0}{(\delta+d)} & \frac{\kappa I_0}{\zeta-\phi\rho I_0} \\ 0 & 0 & 0 & 0 \\ 0 & 0 & 0 & 0 \\ 0 & 0 & 0 & 0 \end{bmatrix},$$

where $m = \beta + \tau + \sigma + d$, $* = \frac{\alpha I_0}{(\gamma+d)} + \frac{\kappa\xi I_0}{(\gamma+d)(\zeta-\phi\rho I_0)}$.

Therefore, the basic reproduction number R_0 of the model in Eq (3.5) is given by

$$R_0 = \frac{\varepsilon}{(\beta + \tau + \sigma + d)(\mu + d)} \left(\frac{\alpha\beta}{(\gamma + d)} + \frac{\theta_1 \tau}{(\delta + d)} \right) + \frac{\kappa\varepsilon}{\zeta(\mu + d) - \phi\rho\varepsilon}.$$

4.2. Stability of the no-rumor equilibrium point

Theorem 3. *For the model in Eq (3.5), if $R_0 < 1$ and $\zeta > \phi\rho I_0$, then the RFE E_0 is locally asymptotically stable.*

Proof. The Jacobian matrix of the model in Eq (3.5) at E_0 is given by:

$$J = \begin{bmatrix} -(\mu + d) & 0 & -\alpha I_0 & -\theta_1 I_0 & -\kappa I_0 \\ 0 & -m & \alpha I_0 & \theta_1 I_0 & \kappa I_0 \\ 0 & \beta & -(\gamma + d) & 0 & 0 \\ 0 & \tau & 0 & -(\delta + d) & 0 \\ 0 & 0 & \xi & 0 & \phi\rho I_0 - \zeta \end{bmatrix}.$$

Obviously, $\lambda_1 = -(\mu + d)$, and the remaining fourth-order characteristic equation is as follows:

$$\det\begin{bmatrix} -m-\lambda & \alpha I_0 & \theta_1 I_0 & \kappa I_0 \\ \beta & -(\gamma+d)-\lambda & 0 & 0 \\ \tau & 0 & -(\delta+d)-\lambda & 0 \\ 0 & \xi & 0 & \phi\rho I_0 - \zeta - \lambda \end{bmatrix} = 0.$$

The characteristic equation obtained is as follows:

$$P(\lambda) = (\phi\rho I_0 - \zeta - \lambda)[(-m-\lambda)(-(\gamma+d)-\lambda) - \alpha\beta I_0](-(\delta+d)-\lambda).$$

Then

$$\begin{aligned} \lambda_{2,3} &= \frac{-(m+\gamma+d) \pm \sqrt{(m-\gamma-d)^2 + 4\alpha\beta I_0}}{2}, \\ \lambda_4 &= -(\delta+d), \\ \lambda_5 &= \phi\rho I_0 - \zeta. \end{aligned}$$

The eigenvalues include $\lambda_1 = -(\mu+d)$ and $\lambda_4 = -(\delta+d)$. When $R_0 < 1$ and $\zeta > \phi\rho I_0$, all eigenvalues $\lambda_1, \ldots, \lambda_5$ have negative real parts. Physically, this implies that in the absence of a rumor outbreak, the "forgetting" speed of the AI system must exceed the "excitation" speed generated by human activity for the system to remain stable. Conversely, if $R_0 > 1$, then $\lambda_2 > 0$, and E_0 becomes unstable.

Theorem 4. *For the model in Eq* (3.5)*, if $R_0 < 1$, the RFE E_0 is globally asymptotically stable.*

Proof. Let $X(t) = (I(t), L(t), S(t), C(t), A(t))^T$. We construct the following Lyapunov function $V(t)$:

$$V(I, L, S, C, A) = \frac{1}{2}(I - I_0)^2 + \frac{1}{2}L^2 + \frac{1}{2}S^2 + \frac{1}{2}C^2 + \frac{1}{2}A^2.$$

According to the properties of the Caputo fractional derivative, we calculate the fractional derivative of $V(X)$ along the system trajectory:

$$\begin{aligned} D^\alpha V &= (I - I_0)D^\alpha I + LD^\alpha L + SD^\alpha S + CD^\alpha C + AD^\alpha A \\ &= (I - I_0)[\varepsilon - \alpha IS - \theta_1 IC - \kappa AI - (\mu+d)I] \\ &\quad + L[\alpha IS + \theta_1 IC + \kappa AI - (\beta+\tau+\sigma+d)L] \\ &\quad + S[\beta L + \theta_2 SC - (\gamma+d)S] + C[\tau L - \theta_2 SC - (\delta+d)C] \\ &\quad + A(\xi S + \phi\rho AI - \zeta A). \end{aligned} \tag{4.2}$$

By substituting $\varepsilon = (\mu + d)I_0$ into the above equation and performing expansion and simplification, we obtain:

$$D^\alpha V(t) = -(\mu+d)(I - I_0)^2 - (\beta+\tau+\sigma+d)L^2 - (\gamma+d)S^2 - (\delta+d)C^2 - \zeta A^2 + P(X).$$

In this expression, $P(X)$ represents the sum of all cross-terms:

$$
\begin{aligned}
P(X) = & -\alpha ILS - \theta_1 ILC - \kappa ILA - \beta LS - \tau LC - \xi SA - \phi\rho IA^2 \\
& - \alpha I(I - I_0)S - \theta_1 I(I - I_0)C - \kappa I(I - I_0)A \\
& - \theta_2 S^2 C + \theta_2 S C^2.
\end{aligned}
$$

Within the domain of attraction for this system trajectory, there exists a constant $M > 0$ such that $0 \leq I(t) \leq M$. Given the boundedness of the total system population, we can take $M = I_0 + \delta$, where $\delta > 0$ is sufficiently small.

To control these cross-terms, this paper introduces Young's inequality:

$$
xy \leq \frac{\omega x^2}{2} + \frac{y^2}{2\omega}, \forall \omega > 0.
$$

To simplify the analysis, let $\omega = 1$ for all terms. Thus, we have:

$$
|\alpha I(I - I_0)S| \leq \frac{\alpha M}{2}(I - I_0)^2 + \frac{\alpha M}{2} S^2.
$$

The remaining terms follow the same principle. Furthermore, for the trilinear term αILS, we have:

$$
|\alpha ILS| \leq \frac{\alpha^2 I^2 L^2}{2\omega_1} + \frac{\omega_1 S^2}{2}.
$$

The remaining terms follow the same principle. For the bilinear term βLS, we have:

$$
|\beta LS| \leq \frac{\beta^2 L^2}{2\omega_2} + \frac{\omega_2 S^2}{2}.
$$

The remaining terms follow the same principle.

Through the aforementioned process, we can obtain

$$
\begin{aligned}
D^\alpha V \leq & -[(\mu + d) - Q_1](I - I_0)^2 - [(\beta + \tau + \sigma + d) - Q_2]L^2 \\
& - [(\gamma + d) - Q_3]S^2 - [(\delta + d) - Q_4]C^2 - [\zeta - Q_5]A^2,
\end{aligned}
$$

where the auxiliary coefficients Q_i are defined as:

$$
\begin{aligned}
Q_1 &= \frac{M}{2}(\alpha + \theta_1 + \kappa), \\
Q_2 &= \frac{M}{2}(\alpha + \theta_1 + \kappa) + \frac{1}{2}(\beta + \tau), \\
Q_3 &= \alpha M + \frac{1}{2}(\beta + \xi), \\
Q_4 &= \theta_1 M + \frac{\tau}{2}, \\
Q_5 &= \kappa M + \frac{\xi}{2} + \phi\rho M.
\end{aligned}
$$

When $R_0 < 1$, the system parameters satisfy the following sufficient conditions:

$$
(\mu + d) > \frac{M}{2}(\alpha + \theta_1 + \kappa),
$$

$$
\begin{aligned}
(\beta+\tau+\sigma+d) &> \frac{M}{2}(\alpha+\theta_1+\kappa)+\frac{1}{2}(\beta+\tau),\\
(\gamma+d) &> \alpha M+\frac{1}{2}(\beta+\xi),\\
(\delta+d) &> \theta_1 M+\frac{\tau}{2},\\
\zeta &> \kappa M+\frac{\xi}{2}+\phi\rho M.
\end{aligned}
$$

By defining positive constants $\eta_1 = (\mu + d) - Q_1 > 0$, $\eta_2 = (\beta + \tau + \sigma + d) - Q_2 > 0$, $\eta_3 = (\gamma + d) - Q_3 > 0$, $\eta_4 = (\delta + d) - Q_4 > 0$, and $\eta_5 = \zeta - Q_5 > 0$, all cross-terms are completely absorbed by the dominant negative-definite quadratic terms. This leads to the result:

$$
D^{\alpha}V(t) \le -\eta_1(I-I_0)^2-\eta_2L^2-\eta_3S^2-\eta_4C^2-\eta_5A^2 \le 0.
$$

This result indicates that when $R_0 < 1$, $D^{\alpha}V(t) \le 0$. Therefore, the largest invariant set within $\{V(I, L, S, C, A) \in \Omega : D^{\alpha}V(t) \le 0\}$ is the singleton set $\{E_0\}$. According to LaSalle's invariance principle[41], if $R_0 < 1$, then E_0 is globally asymptotically stable within Ω. Although the classical LaSalle invariance principle was originally proposed for integer-order systems, Li and Chen [42] have rigorously extended it to fractional-order differential systems. Their generalized LaSalle invariance theorem demonstrates that under the aforementioned conditions, the largest invariant set satisfying $D^{\alpha}V(t) \le 0$ collapses to the single point $\{E_0\}$, thereby proving that $\{E_0\}$ is globally asymptotically stable within Φ.

4.3. Existence and stability of the positive equilibrium point

Based on the model in Eq (3.5), the positive equilibrium point of the system is denoted as $E^* = (I^*, L^*, S^*, C^*, A^*)$. The components of this equilibrium point are derived as follows:

$$
\begin{aligned}
I^* &= \frac{\varepsilon}{\alpha S^*+\frac{\theta_1\tau S^*(\gamma+d)}{\beta(\delta+d-\theta_2S^*)-\tau\theta_2S^*}+\frac{\kappa\xi S^*}{\zeta-\phi\rho I^*}+\mu+d},\\
L^* &= \frac{(\gamma+d)(\delta+d-\theta_2S^*)}{\beta(\delta+d-\theta_2S^*)-\theta_2\tau S^*}S^*,\\
S^* &= \frac{\beta L^*}{\theta_2C^*+\gamma+d},\\
C^* &= \frac{\tau(\gamma+d)}{\beta(\delta+d-\theta_2S^*)-\theta_2\tau S^*}S^*,\\
A^* &= \frac{\xi S^*}{\zeta-\phi\rho I^*}.
\end{aligned}
$$

Theorem 5. *When the parameters satisfy $\zeta > \phi\rho I_0$, $\delta + d > 0$, and $\beta(\delta + d) > (\beta + \tau)\theta_2 S_{\max}$ (where $I_0 = \frac{\varepsilon}{\mu+d}$ and $S_{\max} = \frac{\delta+d}{\theta_2}$), there exists a unique positive equilibrium point $E^* = (I^*, L^*, S^*, C^*, A^*)$ for the model in Eq (3.5), satisfying $S^* \in (0, \frac{\delta+d}{\theta_2})$.*

Proof. Let $D(S) = \beta(\delta + d - \theta_2 S) - \tau\theta_2 S$. To ensure $L^*, C^* > 0$, it is required that $D(S) > 0$ and $\delta + d - \theta_2 S > 0$, which implies: $S \in (0, S_{\max}), D(S) > 0$.

From the model in Eq (3.5), we have:

$$\varepsilon = I^* \left[\alpha S^* + \frac{\theta_1 \tau(\gamma + d) S^*}{D(S^*)} + \frac{\kappa \xi S^*}{\zeta - \phi \rho I^*} + \mu + d\right], \tag{4.3}$$

and we define the function:

$$f(I^*, S^*) = I^* - \frac{\varepsilon}{\alpha S^* + \frac{\theta_1 \tau(\gamma+d)S^*}{D(S^*)} + \frac{\kappa\xi S^*}{\zeta - \phi\rho I^*} + \mu + d}. \tag{4.4}$$

Then, Eq (4.3) is equivalent to $F(I^*, S^*) = 0$. From the model in Eq (3.5), we also obtain:

$$\alpha IS + \theta_1 IC(S) + \kappa A(I, S) I = (\beta + \tau + \sigma + d)\, L(S), \tag{4.5}$$

where the functional expressions are given by:

$$C(S) = \frac{\tau(\gamma + d)S}{D(S)}, \quad A(I, S) = \frac{\xi S}{\zeta - \phi\rho I}, \quad L(S) = \frac{(\gamma + d)(\delta + d - \theta_2 S)}{D(S)} S.$$

Substituting these into Eq (4.5) yields:

$$\alpha IS + \frac{\theta_1 \tau(\gamma + d)\, IS}{D(S)} + \frac{\kappa\xi\, S I}{\zeta - \phi\rho I} = \frac{(\beta + \tau + \sigma + d)(\gamma + d)(\delta + d - \theta_2 S)\, S}{D(S)}. \tag{4.6}$$

For a fixed $S \in (0, S_{\max})$ such that $D(S) > 0$, we define the mapping:

$$T_s(I) = \frac{\varepsilon}{\alpha S + \frac{\theta_1 \tau(\gamma+d)S}{D(S)} + \frac{\kappa\xi S}{\zeta - \phi\rho I} + \mu + d}. \tag{4.7}$$

The derivative of $T_s(I)$ is given by:

$$T_s'(I) = \varepsilon \cdot \frac{\kappa\xi S\, \phi\rho/(\zeta - \phi\rho I)^2}{\left[\alpha S + \frac{\theta_1 \tau(\gamma+d)S}{D(S)} + \frac{\kappa\xi S}{\zeta - \phi\rho I} + \mu + d\right]^2} > 0.$$

Thus, $T_s(I)$ is strictly monotonically increasing. Furthermore, at the boundary values: $T_s(0) = \frac{\varepsilon}{\alpha S + \frac{\theta_1 \tau(\gamma+d)S}{D(S)} + \frac{\kappa\xi S}{\zeta} + \mu + d} > 0$.

As $I \to (\zeta/\phi\rho)^-$, then $T_s(I) \to 0$. Based on strict monotonicity and the intermediate value theorem, there exists a unique fixed point $I = h(S)$. According to the implicit function theorem, $h(S)$ is continuous and differentiable. By differentiating $F(h(S), S) = 0$, we obtain:

$$h'(S) = -\frac{\partial F/\partial S}{\partial F/\partial I} < 0.$$

Consequently, $\partial F/\partial S > 0$ and $\partial F/\partial I > 0$. By substituting $I = h(S)$ into Eq (4.6), we define the following function:

$$\begin{aligned} H(S) = \alpha\, h(S)\, S + \frac{\theta_1 \tau(\gamma + d)\, h(S)\, S}{D(S)} + \frac{\kappa\xi\, S\, h(S)}{\zeta - \phi\rho h(S)} \\ - \frac{(\beta + \tau + \sigma + d)(\gamma + d)(\delta + d - \theta_2 S)\, S}{D(S)}. \end{aligned} \tag{4.8}$$

Equation (4.6) is equivalent to $H(S) = 0$.

Therefore, proving the existence of a unique positive equilibrium point reduces to proving that the equation $H(S) = 0$ has a unique solution within the interval $\{S \in (0, S_{\max}) : D(S) > 0\}$.

Let the interval be denoted as $J = (0, \min\{S_{\max}, S_D\})$, where S_D satisfies $D(S_D) = 0$. Given the condition $\beta(\delta + d) > (\beta + \tau)\theta_2 S_{\max}$, it follows that $J = (0, S_{\max})$.

As $S \to 0^+$, we obtain:

$$h(0^+) = I_0 = \frac{\varepsilon}{\mu + d} D(S) \to \beta(\delta + d) > 0 C(S) \sim \frac{\tau(\gamma + d)}{\beta(\delta + d)} S.$$

Substituting these values into Eq (4.8) yields:

$$H(S) = \left[\frac{\theta_1 \tau(\gamma + d) I_0}{\beta(\delta + d)}\right] S > 0.$$

Thus, there exists $\delta_1 > 0$ such that $H(S) > 0$ for all $S \in (0, \delta_1)$. Similarly, as $S \to S_{\max}^-$, we observe that $\delta + d - \theta_2 S \to 0^+$, $D(S) \to -\tau\theta_2 S_{\max} < 0$, and $h(S) \to 0^+$.

Consequently, the function satisfies:

$$H(S) \to -\varepsilon < 0.$$

Based on the continuity of the function, there must exist at least one $S^* \in (0, S_{\max})$ such that $H(S^*) = 0$. To establish uniqueness, we examine the derivative $H'(S)$:

$$\begin{aligned} H'(S) = {} & \alpha[h(S) + S h'(S)] + \theta_1 \tau(\gamma + d)\left[\frac{h(S) + S h'(S)}{D(S)} - \frac{h(S) S D'(S)}{D^2(S)}\right] \\ & + \kappa\xi\left[\frac{(h(S) + S h'(S))(\zeta - \phi\rho h(S)) + \phi\rho S h(S) h'(S)}{(\zeta - \phi\rho h(S))^2}\right] \\ & - (\beta + \tau + \sigma + d)(\gamma + d)\left[\frac{(\delta + d - \theta_2 S) + S(-\theta_2)}{D(S)} - \frac{(\delta + d - \theta_2 S) S D'(S)}{D^2(S)}\right], \end{aligned}$$

where $D'(S) = -\beta\theta_2 - \tau\theta_2 < 0$. It can be shown that $H'(S) < 0$ throughout the interval; thus, $H(S)$ is strictly monotonically decreasing, ensuring that the equation $H(S) = 0$ has at most one solution.

In summary, given both existence and uniqueness, the model in Eq (3.5) possesses a unique positive equilibrium point E^*. The physical interpretations of the required conditions are as follows: The condition $\zeta > \phi\rho I_0$ ensures that AI activity does not undergo self-reinforcing growth in a rumor-free state, which aligns with the realistic setting of AI as an auxiliary tool rather than an autonomous source of propagation. The condition $\delta + d > 0$ is a natural assumption, indicating that clarifiers will eventually exit the system over time. The condition $\beta(\delta + d) > (\beta + \tau)\theta_2 S_{\max}$ ensures that both clarifiers and latent users maintain positive values at equilibrium, meaning the clarification mechanism is not completely suppressed by rumor propagation.

Theorem 6. *When $R_0 > 1$, the positive equilibrium point E^* is locally asymptotically stable. (Refer to Appendix for the detailed proof).*

4.4. Global asymptotic stability of the positive equilibrium point

Theorem 7. *When $R_0 > 1$, the positive equilibrium point E^* is globally asymptotically stable.*

Proof. Let $X(t) = (I^*, L^*, S^*, C^*, A^*)^T$. Based on Lyapunov stability theory, we construct the following global Lyapunov function $V^*(t)$:

$$\begin{aligned} V^*(t) = &\left(I - I^* - I^* \ln \frac{I}{I^*}\right) + \left(L - L^* - L^* \ln \frac{L}{L^*}\right) + \left(S - S^* - S^* \ln \frac{S}{S^*}\right) \\ &+ \left(C - C^* - C^* \ln \frac{C}{C^*}\right) + \left(A - A^* - A^* \ln \frac{A}{A^*}\right). \end{aligned}$$

Calculating the fractional derivative of $V^*(t)$:

$$\begin{aligned} D^\alpha V^*(t) = &D^\alpha\Bigg[\left(I - I^* - I^* \ln \frac{I}{I^*}\right) + \left(L - L^* - L^* \ln \frac{L}{L^*}\right) + \left(S - S^* - S^* \ln \frac{S}{S^*}\right) \\ &+ \left(C - C^* - C^* \ln \frac{C}{C^*}\right) + \left(A - A^* - A^* \ln \frac{A}{A^*}\right)\Bigg] \\ \leq &\left(1 - \frac{I^*}{I}\right) D^\alpha I + \left(1 - \frac{L^*}{L}\right) D^\alpha L + \left(1 - \frac{S^*}{S}\right) D^\alpha S \\ &+ \left(1 - \frac{C^*}{C}\right) D^\alpha C + \left(1 - \frac{A^*}{A}\right) D^\alpha A \\ = &\left(1 - \frac{I^*}{I}\right)[\varepsilon - \alpha IS - \theta_1 IC - \kappa AI - (\mu + d)I] \\ &+ \left(1 - \frac{L^*}{L}\right)[\alpha IS + \theta_1 IC + \kappa AI - (\beta + \tau + \sigma + d)L] \\ &+ \left(1 - \frac{S^*}{S}\right)[\beta L + \theta_2 SC - (\gamma + d)S] + \left(1 - \frac{C^*}{C}\right)[\tau L - \theta_2 SC - (\delta + d)C] \\ &+ \left(1 - \frac{A^*}{A}\right)(\xi S + \phi\rho AI - \zeta A). \end{aligned} \tag{4.9}$$

According to the equilibrium conditions for the positive equilibrium point:

$$\begin{aligned} \varepsilon &= \alpha I^* S^* + \theta_1 I^* C^* + \kappa A^* I^* + (\mu + d)I^*, \\ \alpha I^* S^* + \kappa I^* A^* + \theta_1 I^* C^* &= (\beta + \tau + \sigma + d)L^*, \\ \beta L^* &= \theta_2 S^* C^* + (\gamma + d)S^*, \\ \tau L^* + \theta_2 S^* C^* &= (\delta + d)C^*, \\ \xi S^* &= \zeta A^* - \phi\rho A^* I^*. \end{aligned}$$

Substituting the first term of Eq (4.9), we obtain:

$$\left(1-\frac{I^*}{I}\right)[\varepsilon-\alpha IS-\theta_1 IC-\kappa AI-(\mu+d)I]$$
$$=\left(1-\frac{I^*}{I}\right)[\alpha I^*S^*+\theta_1 I^*C^*+\kappa A^*I^*-\alpha IS-\theta_1 IC-\kappa AI]$$
$$=\alpha I^*S^*\left(1-\frac{I^*}{I}-\frac{IS}{I^*S^*}+\frac{S}{S^*}\right)$$
$$+\theta_1 I^*C^*\left(1-\frac{I^*}{I}-\frac{IC}{I^*C^*}+\frac{C}{C^*}\right)$$
$$+\kappa A^*I^*\left(1-\frac{I^*}{I}-\frac{IA}{I^*A^*}+\frac{A}{A^*}\right).$$

By utilizing the logarithmic inequality $1-y+\ln y\leq 0$, it can be proven that:

$$\alpha I^*S^*\left(-\ln\frac{I}{I^*}-\ln\frac{S}{S^*}+\ln\frac{IS}{I^*S^*}\right)\leq 0.$$

The remaining terms follow the same logic. Consequently, by summing the expanded forms of all terms and applying both the logarithmic inequality and the arithmetic mean-geometric mean (AM-GM) inequality, we obtain:

$$D^\alpha V\leq -c_I\left(\sqrt{\frac{I}{I^*}}-\sqrt{\frac{I^*}{I}}\right)^2-c_L\left(\sqrt{\frac{L}{L^*}}-\sqrt{\frac{L^*}{L}}\right)^2$$
$$-c_S\left(\sqrt{\frac{S}{S^*}}-\sqrt{\frac{S^*}{S}}\right)^2-c_C\left(\sqrt{\frac{C}{C^*}}-\sqrt{\frac{C^*}{C}}\right)^2-c_A\left(\sqrt{\frac{A}{A^*}}-\sqrt{\frac{A^*}{A}}\right)^2\leq 0,$$

where $c_i\,(i=I,L,S,C,A)$ are positive constants.

In summary, when $R_0>1$, we have $D^\alpha V^*(t)\leq 0$. Thus, $V^*(t)$ is bounded and non-increasing. Furthermore, as $t\to\infty$, the limit of $V^*(t)$ exists. Moreover, $D^\alpha V^*(t)=0$ if and only if $I=I^*$, $L=L^*$, $S=S^*$, $C=C^*$, and $A=A^*$. Therefore, the largest invariant set within $\{(I^*,L^*,S^*,C^*,A^*)\in\Omega^*:D^\alpha V^*(t)=0\}$ is the singleton set $\{E^*\}$. According to LaSalle's invariance principle, all solutions in Ω^* converge to E^*. Consequently, when $R_0>1$, the positive equilibrium point E^* of the model in Eq (3.5) is globally asymptotically stable.

5. Fractional-order optimal control

$u_1(t)$ represents the intensity of measures aimed at suppressing the probability of rumor transmission, including public education and awareness campaigns, preemptive science communication, risk alerts, and similar interventions. The second control function, $u_2(t)$, reflects the intensity of measures designed to enhance the overall influence of rumor clarifiers, specifically involving mechanisms such as legal accountability, corrective actions and warnings, as well as fact-checking-based corrections over deletion. The third control function, $u_3(t)$, denotes the intensity of suppression measures targeting AI-assisted automated rumor propagation mechanisms, which include restricting AI's capacity to automatically disseminate false information and reducing

AI-supported amplification for spreaders. This model integrates strategies for short-term suppression, medium-term traceability, and long-term education to minimize the impact of rumor propagation under finite resources, achieving efficient control and long-term stable governance of rumor transmission. Under the implementation of these intervention strategies, a new model in Eq (5.1) is proposed as follows:

$$\begin{cases} D^{\alpha}I(t) = \varepsilon - \alpha(1-u_1)IS - \theta_1 IC - \kappa AI - (\mu + d)I, \\ D^{\alpha}L(t) = \alpha(1-u_1)IS + \theta_1 IC + \kappa AI - (\beta + \tau(1+u_2) + \sigma + d)L, \\ D^{\alpha}S(t) = \beta L - \theta_2(1+u_2)SC - (\gamma + d)S, \\ D^{\alpha}C(t) = \tau(1+u_2)L + \theta_2(1+u_2)SC - (\delta + d)C, \\ D^{\alpha}A(t) = (1-u_3)\xi S + (1-u_3)\phi\rho AI - \zeta A, \\ D^{\alpha}R(t) = \mu I + \sigma L + \gamma S + \delta C - dR. \end{cases} \tag{5.1}$$

Unlike traditional rumor control models that typically employ static weights, this study addresses the “rapid outbreak and high volume” characteristics of AI-driven rumor propagation by introducing key improvements in the construction of the objective function: weighted normalization of heterogeneous variables. Considering the significant order-of-magnitude differences between $S(t)$ and $A(t)$, we introduce balancing weight coefficients ω_1 and ω_2. This weighting process eliminates inconsistencies in dimensions and scales, ensuring that hazard indicators from different dimensions—human transmission and machine popularity—are treated equitably during strategy formulation.

Based on the properties of different governance measures, the control costs are classified into static rigid costs and dynamic opportunity costs.

For popular science education u_1 and legal deterrence u_2, the associated costs mainly arise from administrative procedures, evidence collection, and content production. These measures are characterized by relatively high entry thresholds and fixed resource consumption. Therefore, the corresponding cost coefficients B_1 and B_2 are assumed to be constants. In practice, large-scale public education campaigns (u_1) require broader social coverage and thus incur higher resource consumption than legal deterrence measures (u_2), leading to $B_1 > B_2$. For technical intervention u_3 targeting AI-driven information dissemination, the marginal cost of technical implementation is relatively low. However, sustained algorithmic regulation may gradually reduce user experience and platform engagement, resulting in cumulative opportunity costs over time. To capture this effect, the cost coefficient associated with u_3 is modeled as an exponentially increasing function $B_3(t) = B_{3,0}e^{\rho t}$. The parameter $\rho > 0$ is defined as the time-sensitive factor, which introduces a temporal penalty mechanism into the control framework. This factor reflects the increasing opportunity cost associated with prolonged technical intervention and influences the temporal allocation of control intensity. As a result, different values of ρ may lead to distinct time-dependent control behaviors, whose characteristics are further examined through numerical simulations.

The exponentially increasing intervention cost is motivated by the concept of time-varying costs in optimal control theory [33]. In AI-assisted misinformation environments, delayed intervention often requires substantially greater resources for content monitoring, recommendation adjustment, and corrective actions. As misinformation accumulates through algorithmic amplification and reaches larger audiences, the difficulty and expense of effective governance may increase at an accelerating rate. Therefore, an exponential cost function is adopted to characterize the growing challenge of late-stage rumor control.

In conclusion, the improved fractional-order optimal control objective functional J is defined as:

$$J(u_1, u_2, u_3) = \int_0^T \left(\omega_1 S + \omega_2 A + \frac{B_1}{2}u_1^2 + \frac{B_2}{2}u_2^2 + \frac{B_3(t)}{2}u_3^2\right) dt. \tag{5.2}$$

Theorem 8. *Let*

$$U = \{(u_1, u_2, u_3) : 0 \leq u_i(t) \leq 1, \quad i = 1, 2, 3, \quad t \in [0, T]\}$$

be the admissible control set. Assume that the state variables remain bounded in a positively invariant region Ω*. Then there exists an optimal control*

$$(u_1^*, u_2^*, u_3^*) \in U,$$

such that

$$J(u_1^*, u_2^*, u_3^*) = \min_{(u_1,u_2,u_3)\in U} J(u_1, u_2, u_3).$$

Proof. The admissible control set U is nonempty, closed, and convex because each control variable satisfies

$$0 \leq u_i(t) \leq 1, \qquad i = 1, 2, 3.$$

For any admissible control $(u_1, u_2, u_3) \in U$, the right-hand side of the system in Eq (4.1) is continuous with respect to both the state variables and the control variables. Moreover, it satisfies the local Lipschitz condition with respect to the state variables. Therefore, by the standard existence and uniqueness theorem, the system in Eq (4.1) admits a unique solution corresponding to each admissible control.

Furthermore, since the total population is normalized and the feasible region Ω is positively invariant, all state variables remain bounded on the interval $[0, T]$.

The integrand of the objective functional J is continuous and contains quadratic control terms. Since

$$B_1 > 0, \qquad B_2 > 0, \qquad B_3 > 0,$$

the integrand is convex with respect to the control variables (u_1, u_2, u_3).

Consequently, all assumptions required by the Filippov–Cesari existence theorem are satisfied. Hence, there exists an optimal control

$$(u_1^*, u_2^*, u_3^*) \in U,$$

which minimizes the objective functional J over the admissible control set U.

The initial conditions are non-negative:

$$I(0) = I_0, L(0) = L_0, S(0) = S_0, C(0) = C_0, A(0) = A_0, R(0) = R_0. \tag{5.3}$$

To balance the numerical orders of magnitude of each integral term in the objective functional and prevent any single factor from dominating the optimization process, we introduced weight coefficients to construct the comprehensive objective functional. The goal of this research is to find an optimal control vector (u_1^*, u_2^*, u_3^*) within the admissible control set $U = \{(u_1, u_2, u_3) | 0 < u_1, u_2, u_3 < 1\}$ such that the objective functional J satisfies:

$$J(u_1^*, u_2^*, u_3^*) = \min J(u_1, u_2, u_3).$$

According to optimal control theory, given the boundedness of the model in Eq (5.1) and the convexity of the objective functional with respect to the control variables, the sufficient conditions for the existence of an optimal control are satisfied. Therefore, an optimal solution for this model must exist. To solve this problem, the Lagrangian function is defined as follows:

$$L(\omega_1, \omega_2, \omega_3, u_1, u_2, u_3) = \omega_1 S + \omega_2 A + \frac{B_1}{2} u_1^2 + \frac{B_2}{2} u_2^2 + \frac{B_3(t)}{2} u_3^2.$$

The Hamiltonian function is defined as follows:

$$\begin{aligned} H = {} & \omega_1 S + \omega_2 A + \frac{B_1}{2} u_1^2 + \frac{B_2}{2} u_2^2 + \frac{B_3(t)}{2} u_3^2 \\ & + \lambda_I \left[\varepsilon - \alpha(1 - u_1(t)) IS - \theta_1 IC - \kappa AI - (\mu + d) I\right] \\ & + \lambda_L \left[\alpha(1 - u_1(t)) IS + \theta_1 IC + \kappa AI - (\beta + \tau(1 + u_2(t)) + \sigma + d) L\right] \\ & + \lambda_S \left[\beta L - \theta_2(1 + u_2(t)) SC - (\gamma + d) S\right] \\ & + \lambda_C \left[\tau(1 + u_2(t)) L + \theta_2(1 + u_2(t)) SC - (\delta + d) C\right] \\ & + \lambda_A \left[(1 - u_3(t)) \xi S + (1 - u_3(t)) \phi \rho AI - \zeta A\right] \\ & + \lambda_R \left[\mu I + \sigma L + \gamma S + \delta C - dR\right]. \end{aligned}$$

where $\lambda_I, \lambda_L, \lambda_S, \lambda_C, \lambda_A, \lambda_R$ are the adjoint variables (or co-state variables).

We now proceed to prove the necessary conditions for optimality for the fractional-order model in Eq (5.1). Let $I^*, L^*, S^*, C^*, A^*, R^*$ be the optimal state solutions corresponding to the optimal control variables $(u_1^*(t), u_2^*(t), u_3^*(t))$ for the models in Eqs (3.1) and (5.1). There exist adjoint variables $\lambda_I, \lambda_L, \lambda_S, \lambda_C, \lambda_A, \lambda_R$ that satisfy the following system of fractional-order differential equations:

$$\begin{cases} D^\alpha \lambda_I = \lambda_I[-\alpha(1 - u_1) S - \theta_1 C - \kappa A - (\mu + d)] \\ \qquad + \lambda_L[\alpha(1 - u_1) S + \theta_1 C + \kappa A] + \lambda_A (1 - u_3) \phi \rho A + \lambda_R \mu, \\ D^\alpha \lambda_L = -\lambda_L[\beta + \tau(1 + u_2) + \sigma + d] + \lambda_S \beta + \lambda_C \tau(1 + u_2) + \lambda_R \sigma, \\ D^\alpha \lambda_S = \omega_1 + \lambda_I[-\alpha(1 - u_1) I] + \lambda_L \alpha(1 - u_1) I \\ \qquad - \lambda_S [\theta_2(1 + u_2) C + \gamma + d] + \lambda_C \theta_2(1 + u_2) C + \lambda_A \xi(1 - u_3) + \lambda_R \gamma, \\ D^\alpha \lambda_C = -\lambda_I \theta_1 I + \lambda_L \theta_1 I - \lambda_S \theta_2(1 + u_2) S \\ \qquad + \lambda_C[\theta_2(1 + u_2) S - \delta - d] + \lambda_R \delta, \\ D^\alpha \lambda_A = \omega_2 - \lambda_I \kappa I + \lambda_L \kappa I + \lambda_A[(1 - u_3) \phi \rho I - \zeta], \\ D^\alpha \lambda_R = -\lambda_R d. \end{cases} \tag{5.4}$$

Theorem 9. *There exists an optimal control triplet (u_1^*, u_2^*, u_3^*) that minimizes the objective functional $J(u_1, u_2, u_3)$. The explicit expressions for these optimal control variables are given by:*

$$u_1^* = \max\left\{0, \min\left\{1, \frac{\alpha IS\,[\lambda_L(t) - \lambda_I(t)]}{B_1}\right\}\right\}$$
$$u_2^* = \max\left\{0, \min\left\{1, \frac{\tau L[\lambda_C(t) - \lambda_L(t)] + \theta_2 SC[\lambda_C(t) - \lambda_S(t)]}{B_2}\right\}\right\}$$
$$u_3^* = \max\left\{0, \min\left\{1, \frac{\lambda_A(t)(\xi S + \phi\rho AI)}{B_3(t)}\right\}\right\}.$$

Proof. According to Pontryagin's maximum principle [43], the adjoint system corresponding to the optimal control problem is derived from the partial derivatives of the Hamiltonian function H with respect to the state variables:

$$D^\alpha \lambda_I = -\frac{\partial H}{\partial I}, \quad D^\alpha \lambda_L = -\frac{\partial H}{\partial L}, \quad D^\alpha \lambda_S = -\frac{\partial H}{\partial S},$$
$$D^\alpha \lambda_C = -\frac{\partial H}{\partial C}, \quad D^\alpha \lambda_A = -\frac{\partial H}{\partial A}, \quad D^\alpha \lambda_R = -\frac{\partial H}{\partial R}.$$

The corresponding optimality conditions (control equations) are given by:

$$\frac{\partial H}{\partial u_1} = B_1 u_1 + \alpha IS(\lambda_I - \lambda_L) = 0,$$
$$\frac{\partial H}{\partial u_2} = B_2 u_2 + \tau L(\lambda_C - \lambda_L) + \theta_2 SC(\lambda_C - \lambda_S) = 0,$$
$$\frac{\partial H}{\partial u_3} = B_3 e^{rt} u_3 - \lambda_C(\xi S + \phi\rho AI) = 0.$$

Solving these equations yields:

$$u_1^* = \frac{\alpha IS\,[\lambda_L(t) - \lambda_I(t)]}{B_1},$$
$$u_2^* = -\frac{\tau L[\lambda_C(t) - \lambda_L(t)] + \theta_2 SC[\lambda_C(t) - \lambda_S(t)]}{B_2},$$
$$u_3^* = \frac{\lambda_C(t)(\xi S + \phi\rho AI)}{B_3(t)}.$$

Therefore, the optimal control solutions can be expressed as:

$$u_1^* = \max\left\{0, \min\left\{1, -\frac{\alpha IS\,[\lambda_I(t) - \lambda_L(t)]}{B_1}\right\}\right\},$$
$$u_2^* = \max\left\{0, \min\left\{1, -\frac{\tau L[\lambda_C(t) - \lambda_L(t)] + \theta_2 SC[\lambda_C(t) - \lambda_S(t)]}{B_2}\right\}\right\},$$
$$u_3^* = \max\left\{0, \min\left\{1, \frac{\lambda_C(t)(\xi S + \phi\rho AI)}{B_3(t)}\right\}\right\}.$$

6. Numerical simulation

In this section, numerical experiments are conducted to verify the dynamical properties of the previously proposed fractional-order Ignorant-Latent-Spreader-Clarifier-Removed-AI (ILSCRA) model and to evaluate the effectiveness of optimal control strategies under time-varying cost constraints. In particular, the simulations are designed to examine how the introduction of the time-sensitive factor influences the temporal allocation of different governance measures.

The numerical analysis consists of two main parts. First, the evolutionary trajectories of the system under different threshold conditions are simulated to validate the theoretical results. This part focuses on the asymptotic stability of the rumor-free equilibrium and the positive equilibrium, illustrating the dynamic evolution of the six state variables over time. Second, to assess the impact of time-varying control costs, the system responses under different control schemes are comparatively analyzed, including strategies with static cost coefficients and strategies incorporating time-varying costs for algorithmic intervention. Three representative control combinations (Strategy A, Strategy B, and Strategy C) are considered. By comparing the variation curves of the spreaders S, debunkers C, and AI propagation activity A, together with the dynamic adjustment paths of the control variables (u_1, u_2, u_3), the simulations highlight how time-varying costs induce adaptive, stage-dependent governance behaviors. The results demonstrate that, compared with static strategies, time-varying optimal control achieves more effective rumor suppression and sustained governance performance while avoiding prolonged reliance on algorithmic intervention.

6.1. Numerical simulation without control measures

The numerical solutions for the fractional-order differential equations are obtained using the fractional Euler method. To achieve better simulation results, the initial population sizes are set as $I = 0.95, L = 0.03, S = 0.08, C = 0.02, R = 0.01$, and $A = 0.01$ with reference to [44]. The initial values of the parameters are summarized in Table 2 below:

Table 2. Constant parameter values in the numerical simulation of the model in Eq (5.1).

Parameters	Parameter values	Source of values
β	0.350/day	[44]
ϕ	0.250/day	Assumptions
ρ	0.040/day	[44]
γ	0.080/day	[44]
d	0.010/day	[44]
a	0.300/day	[44]
ε	0.050/day	[44]
σ	0.080/day	[44]
δ	0.350/day	[44]
μ	0.020/day	[44]
ξ	0.400/day	Assumptions
ζ	0.200/day	Assumptions
κ	0.400/day	Assumptions
θ_1	0.250/day	Assumptions
θ_2	0.250/day	Assumptions
τ	0.020/day	Assumptions

For different derivative orders $0 < \alpha \leq 1$, the basic reproduction number is calculated as $R_0 = 0.0758$. Figure 2 illustrates the evolutionary trajectories of the six state variables—Ignorant (I), Latent (L), Spreader (S), Debunker (C), AI Popularity (A), and Recovered (R)—in the model in Eq (3.1) under fractional orders $\alpha = 0.4, 0.6, 0.8, 1.0$. The simulation results indicate that: Memory Effect and Convergence: When $\alpha = 0.4$, the system exhibits a stronger memory effect, leading to a faster convergence toward the rumor-free equilibrium and a shorter duration of rumor propagation. Impact of Derivative Order: As α increases to 1, the memory effect weakens, and the rate of rumor dissipation slows down, although the system still ultimately tends toward the rumor-free equilibrium. Cumulative Influence: Larger values of α represent a stronger cumulative effect of historical propagation behavior, which results in a decrease in the rate of rumor extinction.

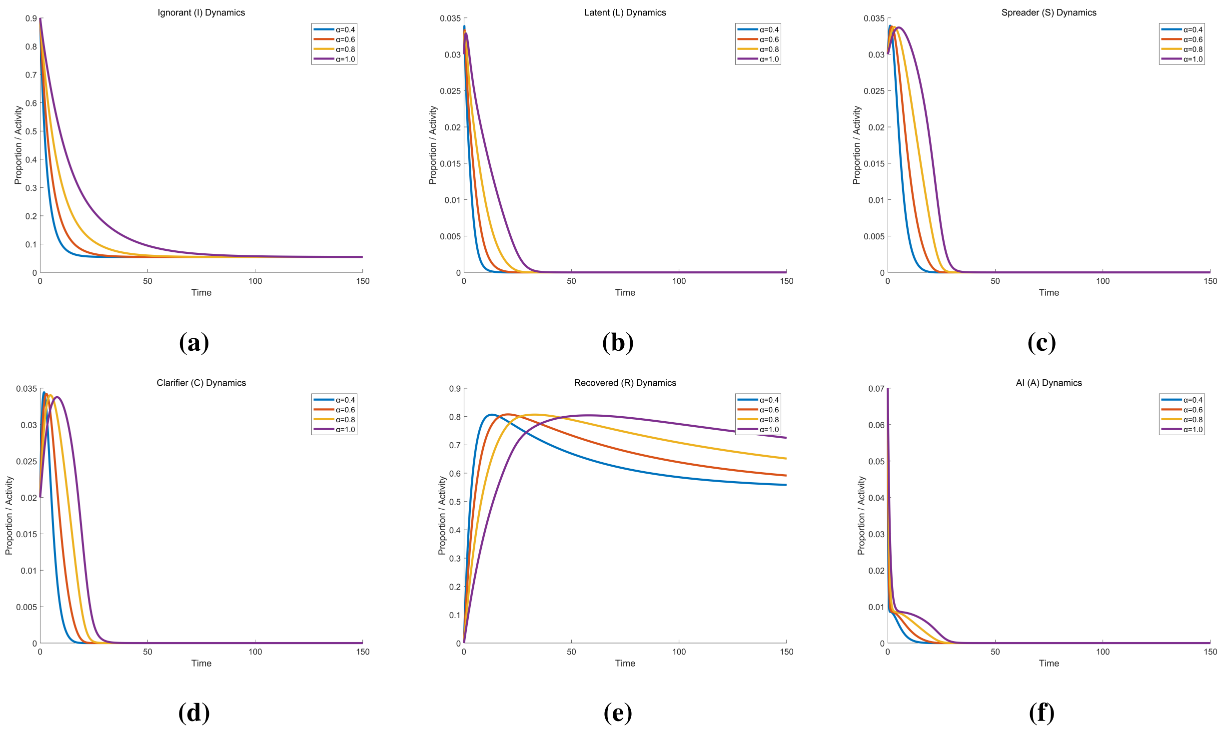

Figure 2. Dynamical behavior of $I(t), L(t), S(t), C(t), R(t), A(t)$ at E_0.

To investigate the influence of memory effects on rumor propagation dynamics, numerical simulations under different fractional orders α are further conducted. The classical integer-order system corresponds to the special case $\alpha = 1$, while smaller values of α represent stronger historical dependence and memory persistence.

The simulation results indicate that decreasing α significantly slows the outbreak speed of rumor-spreaders while simultaneously prolonging the propagation duration. Compared with the integer-order system, the fractional-order model exhibits delayed attenuation and longer spreading tails, which are consistent with persistent recommendation effects commonly observed in AI-assisted online platforms. In particular, historical interaction records continuously influence future recommendation behaviors, causing misinformation to remain active within the information ecosystem for extended periods.

When rumor propagation reaches its peak, the basic reproduction number is calculated as

$R_0 = 17.6251$. The simulation results for this scenario are shown in Figure 3. The analysis reveals that: Effect of Order $\alpha = 0.4$. When the fractional order is $\alpha = 0.4$, the memory effect is prominent, causing the system to converge to the positive equilibrium (endemic equilibrium) relatively quickly and reducing the time required to reach a stable state. Effect of Order $\alpha = 1$: When the fractional order is $\alpha = 1$, the memory effect weakens, resulting in a slower convergence process toward the positive equilibrium and an extended duration of rumor propagation. Impact of Memory Effect: In the vicinity of the positive equilibrium, the memory effect of the fractional-order model is characterized by a greater cumulative influence of early propagation behaviors on the current state, which ultimately shortens the continuous duration of the rumor spread.

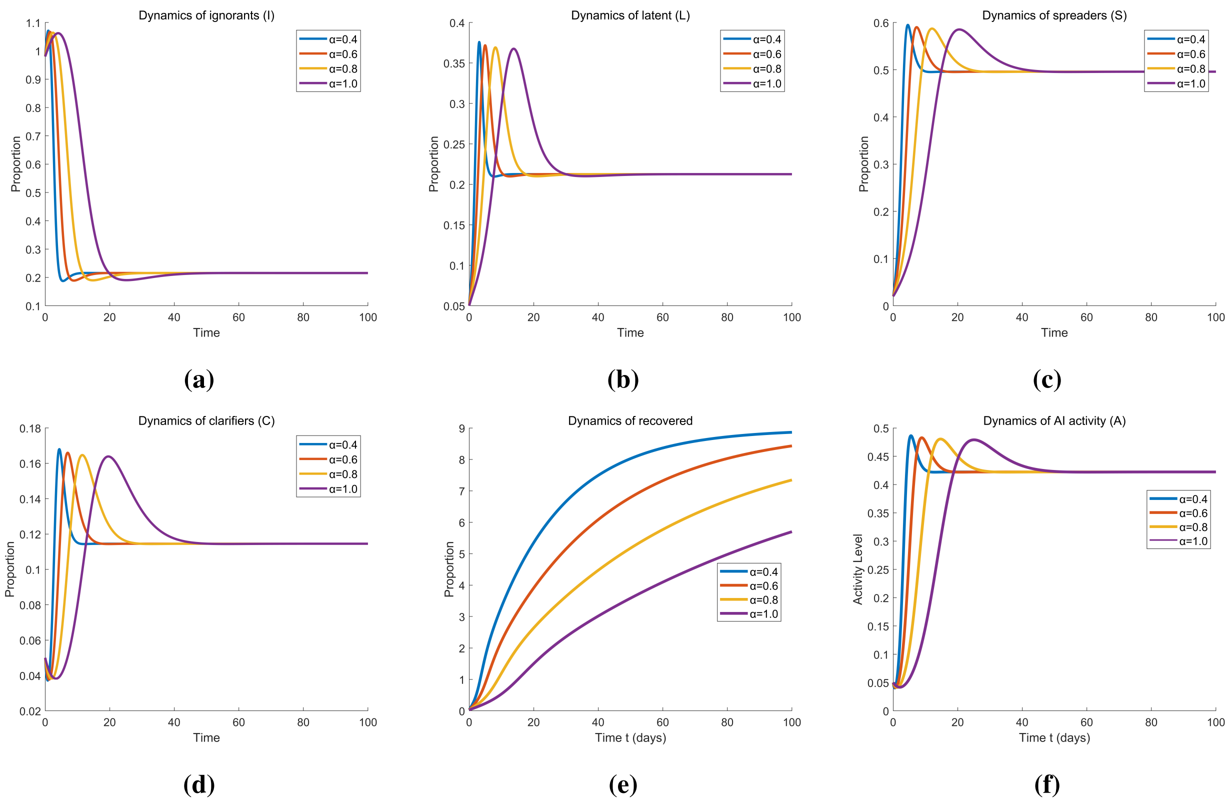

Figure 3. Dynamical behavior of $I(t), L(t), S(t), C(t), R(t), A(t)$ at the equilibrium E^*.

These findings suggest that the fractional-order framework is capable of capturing long-range temporal dependence and repeated exposure phenomena that cannot be adequately represented by classical integer-order models. Therefore, the Caputo fractional model provides a more realistic and effective mathematical framework for analyzing rumor propagation under intelligent recommendation mechanisms.

6.2. *Static parallel control strategies*

To explore the independent effects and synergistic mechanisms of different intervention measures, this section first examines the control performance of three single and combined strategies under the setting of a static cost weight $\rho = 0$. Based on the objective function defined in Section 5 , the criterion for evaluating the strategies is strictly defined as "the ability to minimize the number of spreaders and

AI popularity at the lowest cost".

In this subsection, we assume that the cost of algorithmic control is constant, i.e., the time-sensitive factor is set to ρ, such that $B_3(t) = b_{B,0}$. We solve the fractional-order model numerically using the Grunwald–Letnikov method and investigate the effectiveness of the optimal control strategies. For the fractional derivative $D^{\alpha}x(t)$, its discretization can be expressed as:

$$D^{\alpha}x(t) \approx \frac{1}{h^{\alpha}}\sum_{k=0}^{N}(-1)^{k}\binom{\alpha}{k}x(t-kh),$$

where h is the time step and N is the maximum order of time discretization. The term $\binom{\alpha}{k} = \frac{\Gamma(\alpha+1)}{\Gamma(k+1)\Gamma(\alpha-k+1)}$ represents the generalized binomial coefficient. Figure 4(a)–(f) illustrates the comparison before and after the implementation of control measures. The final time T is set to 150 days.

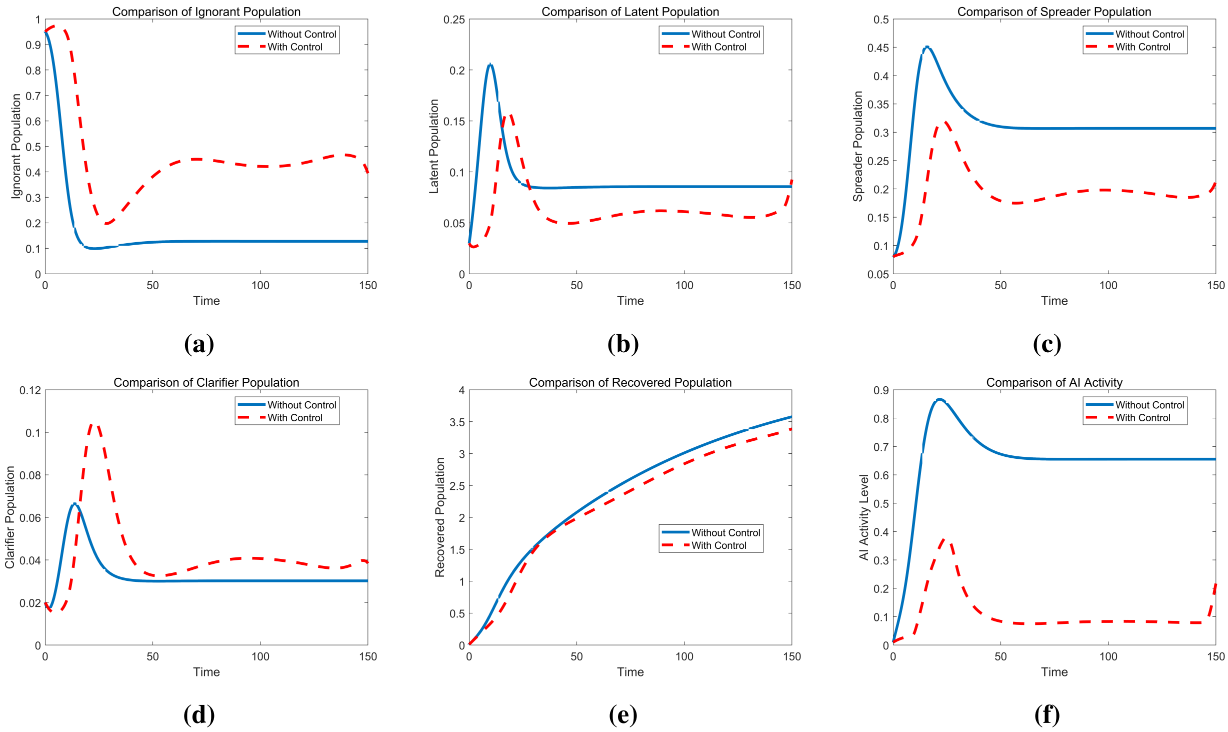

Figure 4. Comparison of population changes before and after the implementation of control measures.

Based on the simulation results in Figure 4, the advantages of the model after implementing control measures are reflected in the following aspects:

Suppression of Propagation Peaks: The peak of rumor propagation is controlled at an earlier stage with a significantly reduced magnitude. This avoids the emergence of a peak period, thereby mitigating the substantial impact on society.

Acceleration of Rumor Dissipation: The control measures accelerate the decay process of rumors, allowing them to subside within a shorter timeframe and preventing long-term propagation.

Optimization of Population Distribution: Following the intervention, the number of spreaders S is significantly reduced, while the number of debunkers C increases substantially.

The fractional-order model with control integrated demonstrates superior performance in managing the propagation speed, scope of influence, and duration of rumors, indicating significant practical application value.

Figure 5 compares the system dynamics under integer-order ($\alpha = 1.0$) and fractional-order ($\alpha = 0.60$) control. The integer-order trajectory smooths out relatively quickly but traps the system in a high steady state, with the proportion of spreaders stagnating above 0.25. This indicates a clear bottleneck where traditional memoryless interventions fail to further eliminate the rumor. The fractional-order model, however, leverages the system's memory to accumulate suppression force over time. Although it exhibits a higher initial peak—accurately reflecting the rapid initial burst of AI algorithmic amplification—the historical accumulation of control measures eventually drives the propagation scale down to a much deeper trough (near 0.1 around $t = 45$). This result demonstrates that fractional-order control can break the high-level stagnation typical of integer models, achieving a more thorough and deeper suppression of persistent AI-driven rumors.

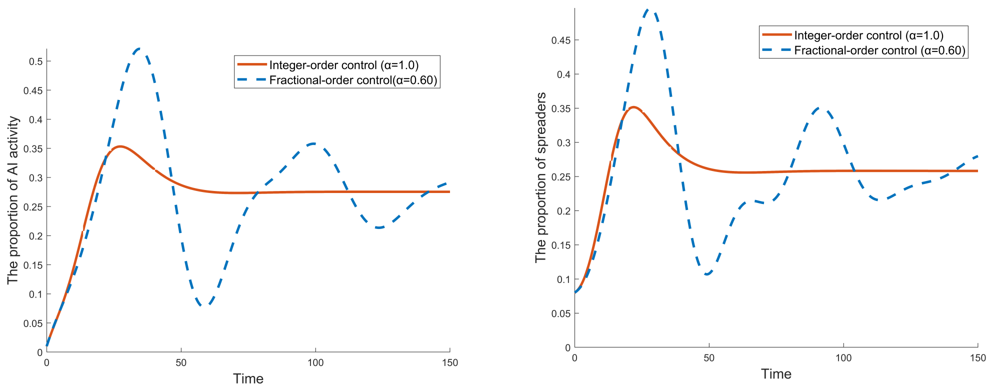

(a) AI transmission activity **(b)** Proportion of spreaders

Figure 5. Comparison of system dynamics under fractional-order ($\alpha = 0.60$) and integer-order ($\alpha = 1.0$) control strategies.

To further identify the most efficient approach, we compare the following three control strategies:

Strategy A: Legal Punishment + Platform Traffic Restriction (u_1, u_3).

Strategy B: Incentive Mechanism (u_2).

Strategy C: Legal Punishment + Incentive Mechanism + Platform Traffic Restriction (u_1, u_2, u_3).

The number of rumor-spreaders, the number of clarifiers, and the AI transmission activity under Strategies A to C are shown in (a)–(c) of Figure 6, respectively. In terms of controlling the scale of rumor-spreaders, Strategy C demonstrates the most significant effect. It not only substantially reduces the peak number of spreaders during the outbreak (from approximately 0.45 to around 0.33) but also significantly lowers the proportion of spreaders at the final steady state. On the other hand, the number of clarifiers under Strategy C shows a sharp increase, with its peak significantly higher than those under Strategies A and B, and maintains a higher population density at the steady state. Regarding the variation in AI transmission activity, Strategy C effectively suppresses the peak AI activity and controls its steady-state level within a lower range (approximately 0.48). This indicates that relying solely on punitive measures or solely on incentives has limited effectiveness, whereas a comprehensive multi-pronged governance approach can more effectively curb rumor dissemination.

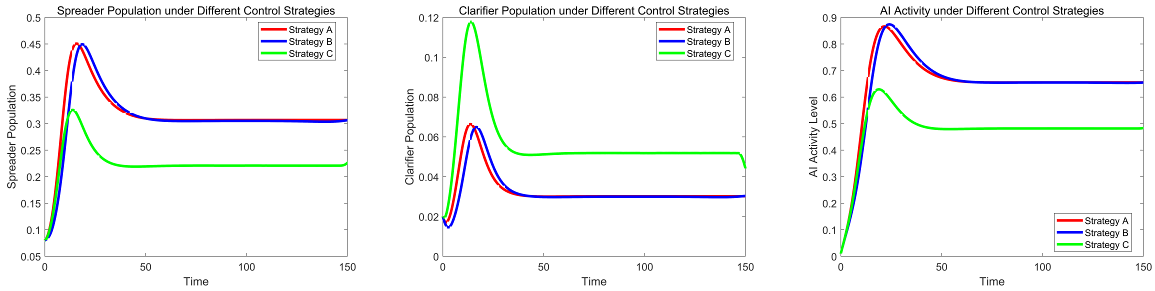

(a) Variable $S(t)$ **(b)** Variable $C(t)$ **(c)** Variable $A(t)$

Figure 6. Simulation results of Strategy A to Strategy C: (a) total number of rumor-spreaders; (b) total number of clarifiers; (c) AI transmission activity.

However, considering the high execution costs associated with the implementation of multiple overlapping control measures, there is a need to further explore how to optimize resource allocation over the time dimension to achieve the best balance between governance effectiveness and economic cost. This leads to the discussion on time-varying optimal control in the next section.

Figure 7 illustrates the optimal control trajectories for Strategies A to C.

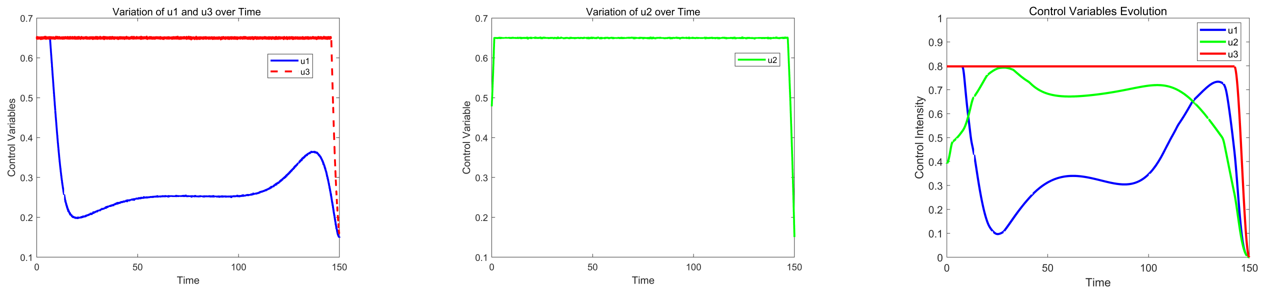

(a) Strategy A **(b)** Strategy B **(c)** Strategy C

Figure 7. Optimal control strategies under Strategies A, B, and C.

6.3. *Optimal governance strategy under time-varying control costs*

This section focuses on how the time-sensitivity factor ρ influences the temporal allocation of control efforts under time-varying costs, thereby shaping the optimal governance strategy for AI-driven rumor propagation. To simulate realistic governance constraints, the target weights are set as $\omega_1 = 5$ and $\omega_2 = 0.5$. A cost hierarchy is constructed according to the implementation thresholds of different governance measures, with $B_1 = 3 > B_2 = 2 > B_3 = 0.5$. This setting reflects practical considerations, where legal regulation involves relatively high administrative barriers, while algorithmic intervention typically exhibits lower marginal costs.

6.3.1. *Pareto frontier analysis of the time-sensitivity factor ρ*

In the objective function, the time-sensitivity factor ρ is a core parameter that determines the intensity of the control strategy. To determine the optimal value of ρ, rather than relying on subjective settings, this study performs a parameter sensitivity analysis for ρ within the interval $[0.1, 1.5]$ and constructs a Pareto frontier between governance costs and social harm.

As illustrated in Figure 8, the cost-harm trade-off curve of the system exhibits a prominent L-shaped Pareto frontier, which intuitively reveals the law of diminishing marginal utility in governance effectiveness. Based on the quantitative data analysis in Table 3 and the swept view of Figure 9, the parameter selection process is categorized into two distinct stages:

High-Return Zone ($0 < \rho < 0.8$): In this interval, the curve descends steeply along the left side, indicating that increasing the time-sensitivity factor can achieve significant harm reduction at a relatively low incremental cost. Data from Table 3 shows that when ρ increases from 0.6 to 0.8, the marginal governance utility maintains an effective level of 0.14. This implies that early intervention measures, such as legal deterrence and popular science education, can precisely target the rumor propagation chain, placing the strategy in a "high-efficiency" phase. Diminishing Returns Zone ($0.8 < \rho < 1.5$): Once ρ exceeds 0.8, the system's effectiveness experiences a precipitous decline. Constrained by the exponential growth characteristic of the opportunity cost function e^{ρ}, governance costs escalate sharply while the total social harm remains nearly stagnant. At this stage, the marginal utility plummets toward 0.01 or even approaches zero, trapping the system in a "high-consumption, low-efficiency" involutionary trap. Consequently, at $\rho = 0.8$, the system achieves the optimal marginal balance between "control cost investment" and "harm reduction effectiveness". Therefore, $\rho = 0.8$ is selected as the optimal parameter for subsequent time-varying control analysis, while other cost coefficients ($B_1 = 3 > B_2 = 2 > B_3 = 0.5$) remain constant.

Figure 9 plots the continuous scanning trajectories of the system state as it varies with the time-sensitivity factor ρ. Geometrically, the red star corresponds to the position with the maximum curvature of the objective function, indicating that truncating the scan at this point can maximize the suppression of resource consumption while ensuring the effectiveness of harm control.

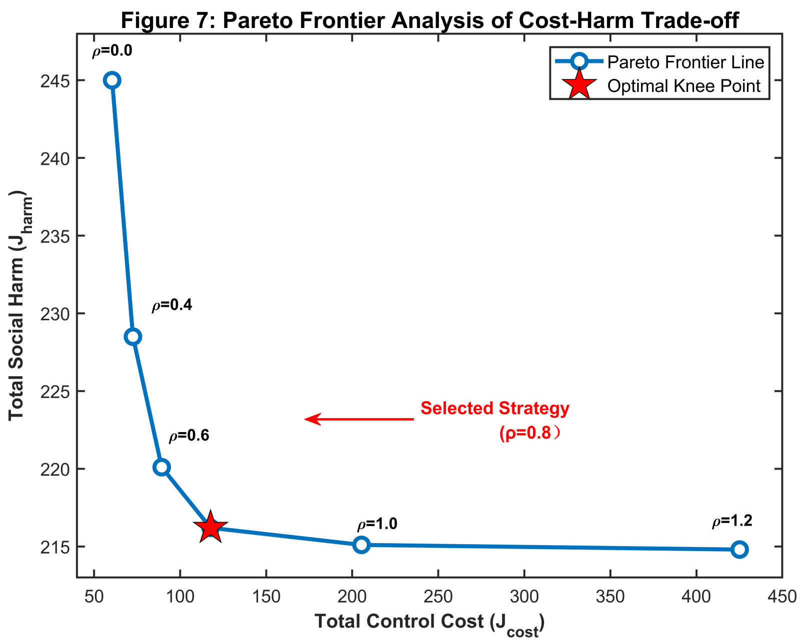

Figure 8. Cost-hazard trade-off analysis under different ρ-values.

Table 3. Comparison of governance effectiveness indicators under different time-sensitivity factors ρ.

ρ	Total Control Cost	Total Social Harm	Cost Growth Rate	Harm Reduction Rate	Marginal Utility	Remarks
0.0	60.5	245.0	–	–	–	Baseline
0.4	72.6	228.5	+20.5%	−6.7%	1.363	Initial Success
0.6	89.3	220.1	+23.0%	−3.7%	0.503	High Return
0.8	117.7	216.2	+31.8%	−1.8%	0.137	Optimal Inflection Point
1.0	205.4	215.1	+74.5%	−0.5%	0.012	Diminishing Returns
1.2	425.1	214.8	+107.0%	−0.1%	0.001	Significant Loss

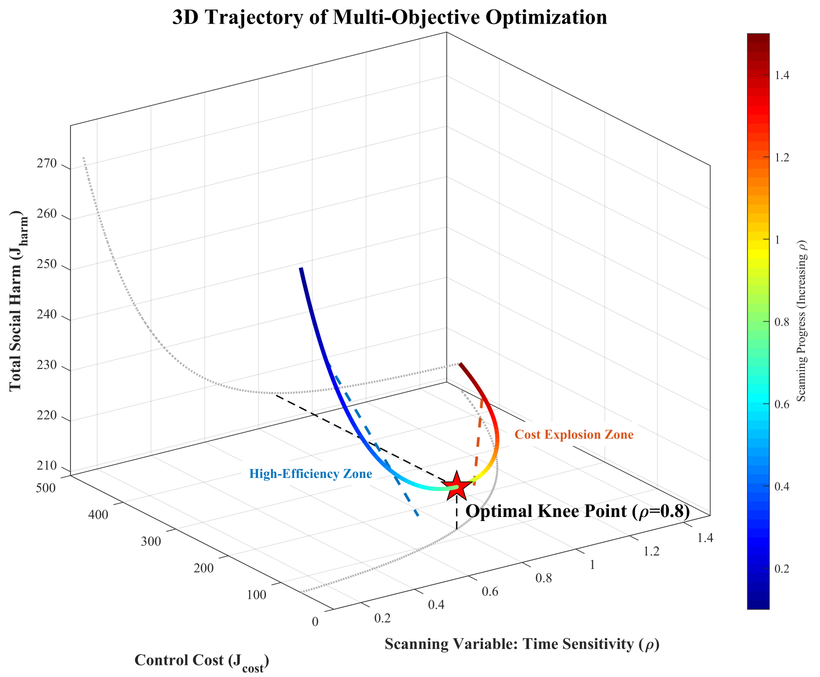

Figure 9. Multi-objective optimization of three-dimensional trajectory and identification of optimal turning points for cost control and social harm mitigation.

To eliminate the potential interference of weight selection on the identification of the optimal solution, Figure 10 constructs a global objective function surface within a dual-parameter space. The red dashed line in Figure 10 traces the distribution trajectory of the optimal ρ value as ω_2 varies continuously from 0.1 to 1.0. The analytical results indicate the following: as ω_2 increases, the overall comprehensive cost of the system rises accordingly. Crucially, the projection of the red trajectory on the horizontal plane remains consistently stable near $\rho \approx 0.8$, without exhibiting any significant lateral drift. This result demonstrates that the selection of the optimal control parameter ρ is insensitive to the weight ω_2. Regardless of how the potential harm level of AI is assessed, $\rho = 0.8$ consistently remains the optimal solution under the current dynamical constraints. This underscores the strong structural robustness of the proposed control strategy.

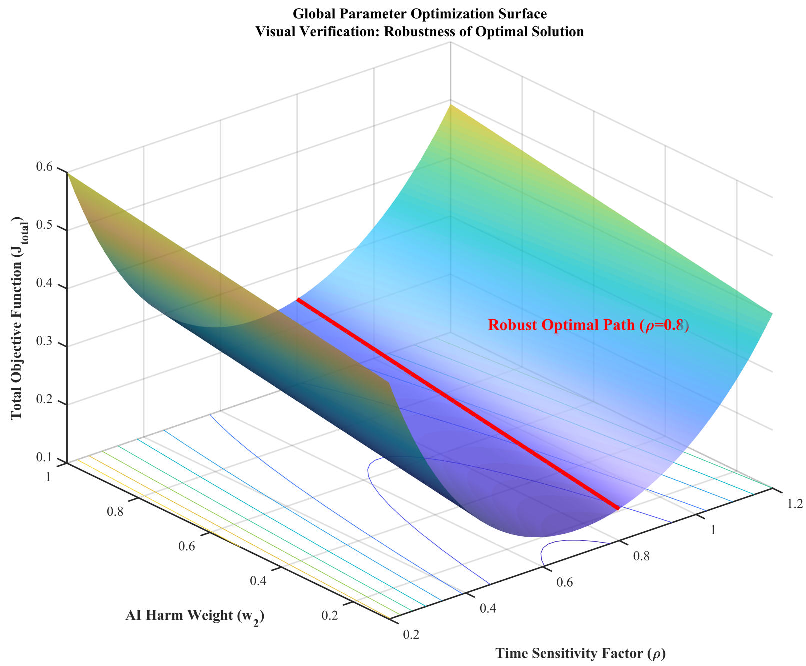

Figure 10. Parameter optimization trajectory based on spatio-temporal scanning: Geometric boundary between high-efficiency areas and areas with escalating costs.

6.3.2. Comparison and analysis of control strategies: A slow-fast coupled governance framework

To verify the effectiveness of the proposed slow-fast coupling mechanism in rumor governance, Figure 11 compares the evolutionary trajectories of the control variables under static and time-varying control strategies. The simulation results can be summarized as follows.

Static strategy performance: As illustrated in Figure 11(a), under static weight settings, the control variables exhibit poor temporal adaptability to the evolution of rumor-spreading. In particular, algorithm-based suppression u_3 (red), representing platform-level content blocking and recommendation restriction, remains at its upper saturation level (0.8) for nearly the entire simulation horizon ($0 < t < 145$), regardless of the actual attenuation of rumor diffusion. Meanwhile, legal accountability u_2 (green) is maintained at a high intensity between $t = 20$ and $t = 120$. The long-term coexistence of multiple high-intensity interventions indicates substantial redundancy in rumor governance, as costly technical suppression is not relaxed even after the rumor has effectively lost its propagation momentum. Time-varying strategy performance: As shown in Figure 11(b), introducing time-varying control costs leads to a clear time-scale separation among different rumor intervention measures. The overall rumor governance process can be divided into three distinct stages according to the dominant control mechanism.

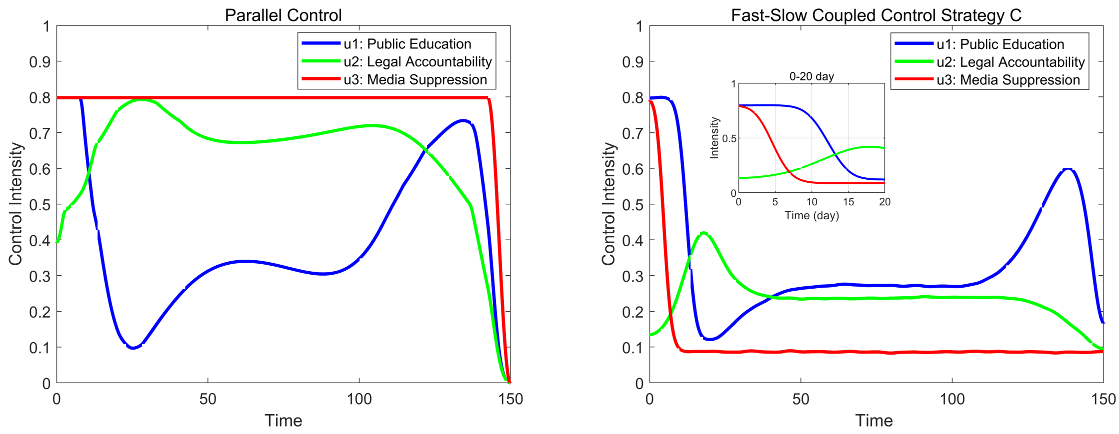

(a) **(b)**

Figure 11. Comparison of control trajectories under different cost strategies: (a) static parallel control ($\rho = 0$); (b) fast-slow coupling control ($\rho = 0.8$).

Phase I ($0 < t < 10$): During the initial outbreak stage, the algorithmic suppression measure u_3 (red) is activated at a high intensity and implemented in coordination with public education u_1 (blue), jointly containing the explosive growth of rumors in the early phase. Owing to the sharply increasing opportunity cost associated with sustained algorithmic intervention, the intensity of u_3 declines rapidly and approaches the minimum baseline level by $t = 10$. Phase II ($10 < t < 40$): As the effect of algorithmic suppression weakens, the legal accountability measure u_2 (green) intensifies rapidly, reaching its peak around $t \approx 18$. During this stage, u_2 becomes the dominant mechanism for suppressing residual rumor propagation and stabilizing the transitional dynamics of the system. Phase III ($t > 40$): In the mid-to-late control period, the legal measure u_2 (green) gradually shifts to a supporting role, while public education u_1 (blue) becomes dominant. The intensity of u_1 remains at approximately 30% for an extended period and reaches a secondary peak near $t \approx 135$, playing a crucial role in consolidating rumor dissipation and preventing secondary spread.

Overall, the proposed time-varying control strategy achieves an efficient temporal allocation of governance measures through a regulatory structure that couples fast and slow interventions. Specifically, algorithmic suppression dominates the outbreak stage ($0 < t < 10$), legal deterrence governs the transitional stage ($10 < t < 40$), and public education ensures long-term stability during the consolidation stage ($t > 40$). This allocation is realized through a sequential dynamic transition of control measures. As a fast intervention, algorithmic suppression is initially implemented at high intensity to rapidly contain rumor diffusion; however, due to cost considerations, its intensity decays quickly after the early stage and is maintained at a low auxiliary level. This transition releases the dominant role to slower interventions, such as legal accountability and public education, allowing them to successively assume central importance in the medium- and long-term stages. The coordinated handover and synergy among interventions operating at different speeds form a closed-loop dynamic control structure, providing a coherent dynamical framework for staged rumor intervention in AI-driven communication environments.

Figure 12 illustrates the comparison of three key system indicators under a static strategy (fixed weights) versus a time-varying dynamic strategy.

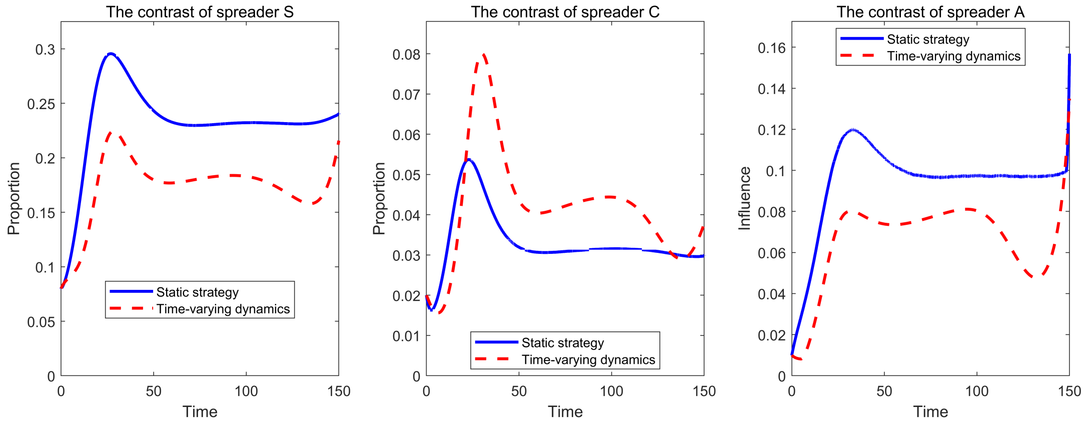

Figure 12. Comparison of system state evolution under different cost strategies: (a) communicator scale $S(t)$; (b) clarifier scale $C(t)$; (c) AI propagation activity $A(t)$.

Comparison of spreaders $S(t)$ (Figure 12(a)): Under the static strategy, the proportion of spreaders rises rapidly, peaking close to 0.3, and subsequently declines slowly, maintaining a relatively high level over the long term. In contrast, the time-varying strategy significantly suppresses the propagation peak to around 0.22 and results in a lower final steady-state level. This indicates that dynamically adjusting control intensity can more effectively contain the overall scale of rumor propagation. Comparison of clarifiers $C(t)$ (Figure 12(b)): The two strategies differ significantly in mobilizing clarifiers. Under the time-varying strategy, the peak proportion of clarifiers is more than double that under the static strategy, and their activity remains relatively high in the later stages of evolution. This suggests that gradually reallocating emphasis toward education and legal measures can encourage sustained user participation in rumor clarification. Comparison of AI propagation activity $A(t)$: (Figure 12(c)): The static strategy exhibits a relatively weak suppression effect on AI activity, with values remaining above 0.1 for an extended period. In contrast, the time-varying strategy applies stronger regulatory intervention during the early stage to reduce AI activity to a low level. Although the control intensity decreases later due to cost constraints, leading to a moderate rebound, the overall activity level remains substantially lower than that under the static strategy, effectively limiting the algorithm's continued amplification of rumors.

The comparative results demonstrate that, compared with the static strategy using fixed inputs, the time-varying strategy—by adjusting governance emphasis across different stages—achieves superior control performance, reducing propagation risks while significantly enhancing clarification efficiency.

Compared with classical rumor propagation models that mainly focus on interpersonal interactions, the proposed model incorporates AI-driven algorithmic amplification, environmental influences, and fractional-order memory effects. The numerical results show that the fractional-order parameter has a significant influence on rumor dynamics, indicating that historical dissemination behaviors play an important role in the spreading process. In addition, the interaction between human spreaders and AI recommendation mechanisms can further enhance rumor persistence and dissemination. The optimal control simulations demonstrate that the proposed intervention strategy effectively reduces the density of spreaders and suppresses rumor propagation. Therefore, the proposed model provides a more realistic framework for describing and controlling rumor dissemination in modern AI-assisted information environments.

7. Conclusions

This paper addresses the issue of online public opinion dissemination in the context of deep AI intervention by constructing a fractional-order dynamical model incorporating an "AI transmission activity" state variable. Unlike traditional approaches that treat algorithmic influence as fixed parameters, this study characterizes algorithmic recommendation as an independent dynamic state variable and incorporates latency and clarification processes. This framework provides a systematic description of the nonlinear coupling between algorithmic behavior and individual dissemination actions.

From a theoretical perspective, the non-negativity and boundedness of the model solutions are established, the basic reproduction number characterizing the threshold property of rumor propagation is derived, and the stability conditions of both rumor-free and positive equilibria are analyzed. These results lay a solid mathematical foundation for subsequent control analysis. Building on this foundation, a fractional-order optimal control problem with time-varying costs is formulated to reflect the dynamic characteristics of AI-driven rumor propagation. The analysis shows that when the cost of algorithmic intervention increases exponentially over time, the optimal control strategy exhibits a distinct stage-dependent adjustment pattern. In the early stage, algorithmic regulation emphasizes intensive intervention to rapidly suppress rumor amplification. As algorithmic costs accumulate, the control focus gradually shifts toward legal accountability in the intermediate stage to maintain deterrence, and further toward public education in the later stage to consolidate long-term stability. This result underscores the inherent limitations of relying solely on technological interventions and provides a theoretical basis for a coordinated governance strategy with prioritized measures.

Numerical simulations further support these theoretical findings. Comparative results demonstrate that rationally coordinated control strategies significantly reduce the peak scale of rumor-spreaders and shorten the attenuation period of public opinion. Moreover, compared with single-dimensional interventions, a comprehensive strategy integrating algorithmic regulation, legal deterrence, and public education achieves superior performance in suppressing rumor dissemination and limiting AI transmission activity, while better balancing governance costs and effectiveness.

In summary, as AI technologies substantially amplify information dissemination efficiency, effective rumor governance requires a systemic perspective. A multi-layered framework should be established by coordinating technological interventions, institutional regulation, and social cognition. Algorithmic regulation plays a crucial role in short-term intensive suppression, legal norms provide mid-term stabilization, and public education forms the foundation for long-term societal resilience. The coordinated synergy of these elements represents a viable pathway toward low-cost and sustainable public opinion governance.

Although the present study mainly focuses on the theoretical analysis of AI-assisted rumor propagation dynamics, incorporating real-world social media dissemination data would further improve the practical applicability of the proposed model. Due to the limited public accessibility of personalized recommendation and historical interaction data from online platforms, real-data-driven parameter estimation was not considered in the current work. In future research, we plan to combine actual social media rumor propagation datasets with the proposed fractional-order framework to further validate the effectiveness and realism of the model.

Use of AI tools declaration

The authors declare they have not used Artificial Intelligence (AI) tools in the creation of this article.

Conflict of interest

The authors declare that they have no conflict of interest. Ethical statements: The authors hereby declare that this manuscript is the result of their independent creation under the reviewers'comments, except for the quoted contents. This manuscript does not contain any research achievements that have been published or written by other individuals or groups. The legal respon- sibility of this statement shall be borne by the authors.

Acknowledgment

The work is supported by the Natural Science Foundation of Shaanxi Province under Project (2023-JC-YB-084).

Author contributions

Conceptualization, L.W. and Z.Y.; Methodology, L.W.; Formal analysis, L.W.; Investigation, L.W.; Validation, L.W.; Resources, Z.Y.; Supervision, Z.Y.; Writing—original draft preparation, L.W.; Writing—review and editing, L.W. and Z.Y. All authors have read and agreed to the published version of the manuscript.

Appendix

Proof of Theorem 6

Proof. The Jacobian matrix at the positive equilibrium point $(I^*, L^*, S^*, C^*, A^*)$ is

$$J = \begin{bmatrix} -\alpha S^* - \theta_1 C^* - \kappa A^* - R_1 & 0 & -\alpha I^* & -\theta_1 I^* & -\kappa I^* \\ \alpha S^* + \theta_1 C^* + \kappa A^* & -R_2 & \alpha I^* & \theta_1 I^* & \kappa I^* \\ 0 & \beta & -\theta_2 C^* - R_3 & -\theta_2 S^* & 0 \\ 0 & \tau & \theta_2 C^* & \theta_2 S^* - R_4 & 0 \\ \phi\rho A^* & 0 & \xi & 0 & \phi\rho I^* - R_5 \end{bmatrix},$$

where $R_1 = \mu + d$, $R_2 = \beta + \tau + \sigma + d$, $R_3 = \gamma + d$, $R_4 = \delta + d$, and $R_5 = \zeta$.

The corresponding characteristic equation is:

$$\lambda^5 + c_1\lambda^4 + c_2\lambda^3 + c_3\lambda^2 + c_4\lambda + c_5 = 0,$$

where

$$c_1 = \kappa A + (\alpha - \theta_2)S^* + \theta_1 C^* - \phi\rho I^* + R_1 + R_2 + R_3 + R_4 + R_5,$$

$$
\begin{aligned}
c_2 = {} & I^*\Big[\phi\rho S^*(\theta_2 - \alpha) - \phi\rho C^*(\theta_1 + \theta_2) - \phi\rho(R_1 + R_2 + R_3 + R_4) - (\alpha\beta + \theta_1\tau)\Big] \\
& + S^*\Big[\alpha(R_1 + R_2 + R_3 + R_4) - \theta_2\kappa A - \theta_2(R_1 + R_2 + R_3 + R_4)\Big] \\
& + C^*\Big[\theta_2\kappa A + (\theta_1 + \theta_2)(R_1 + R_2 + R_3 + R_4)\Big] \\
& + (\alpha - \theta_1)\theta_2 S^* C^* + (R_1 + R_2 + R_3 + R_4)\kappa A \\
& - \alpha\theta_2 S^{*2} + \sum_{1\le i<j\le 5} R_i R_j,
\end{aligned}
$$

$$
\begin{aligned}
c_3 = {} & \phi\rho I^* S^*[\theta_2(\alpha S^* + \theta_1 C^* - \alpha C^*)] - \phi\rho\theta_1\theta_2 I^* C^{*2} \\
& + I^{*2}\phi\rho(\alpha\beta + \theta_1\tau) + C^{*2}\theta_1\theta_2(R_1 + R_4 + R_5) \\
& + \phi\rho I^*\Big[S^*(\theta_2 R_1 + (\theta_2 - \alpha)(R_2 + R_3) - \alpha R_4) \\
& \qquad - C^*(\theta_2 R_1 + (\theta_1 + \theta_2)(R_2 + R_4))\Big] \\
& + \theta_2\kappa A[C^*(R_2 + R_4 + R_5) - S^*(R_2 + R_3 + R_5)] \\
& - \phi\rho I^*[R_1(R_2 + R_3 + R_4) + R_2(R_3 + R_4) + R_3 R_4] \\
& + S^* C^*[\alpha\theta_2(R_2 + R_4 + R_5) - \theta_1\theta_2(R_2 + R_3 + R_5)] \\
& + I^*[\theta_2 S^*(\alpha\beta + \alpha\tau) - \theta_1\theta_2 C^*(\beta + \tau)] \\
& + A\kappa[R_2(R_3 + R_4 + R_5) + R_3(R_4 + R_5) + R_4 R_5] \\
& - I^*[\alpha\beta(R_1 + R_4 + R_5) + \theta_1\tau(R_1 + R_3 + R_5)] \\
& - \beta\xi\kappa I^* \\
& + S^*\Big[\alpha \sum_{2\le i<j\le 5} R_i R_j - \theta_1\big(R_1(R_2 + R_3 + R_5) + R_2(R_3 + R_5) + R_3 R_5\big)\Big] \\
& + C^*\Big[\theta_1 \sum_{2\le i<j\le 5} R_i R_j + \theta_2\big(R_1(R_2 + R_4 + R_5) + R_2(R_4 + R_5) + R_4 R_5\big)\Big] \\
& + \sum_{1\le i<j<k\le 5} R_i R_j R_k,
\end{aligned}
$$

$$
\begin{aligned}
c_4 = {} & \phi\rho I^*\Big\{\alpha\theta_2 S^{*2}(R_2 + R_3) + S^* C^*[\theta_1\theta_2(R_2 + R_3) - \alpha\theta_2(R_2 + R_4)] \\
& \qquad - \theta_1\theta_2 C^{*2}(R_2 + R_4)\Big\} \\
& + \phi\rho I^{*2}\Big[- \theta_1 S^*(\alpha\beta + \alpha\tau) + \theta_2 C^*(\beta + \tau) + \alpha\beta(R_1 + R_4) + \theta_1\tau(R_1 + R_3)\Big] \\
& + \phi\rho I^*\Big\{\theta_2 S^*\Big[R_1(R_2 + R_3) - \alpha(R_2 R_3 + R_2 R_4 + R_3 R_4)\Big] \\
& \qquad - C^*\Big[\theta_2(R_1 R_2 + R_1 R_4 + R_2 R_4) + \theta_1(R_2 R_3 + R_2 R_4 + R_3 R_4)\Big]\Big\}
\end{aligned}
$$

$$
\begin{aligned}
&- \phi\rho I^*\Big[R_1(R_2R_3 + R_2R_4 + R_3R_4) + R_2R_3R_4\Big] \\
&+ \theta_2\kappa A\Big[C^*(R_2R_4 + R_2R_5 + R_4R_5) - S^*(R_2R_3 + R_2R_5 + R_3R_5)\Big] \\
&- \alpha\theta_2 S^*(R_2R_3 + R_2R_5 + R_3R_5) \\
&+ S^*C^*\Big[\alpha\theta_2(R_2R_4 + R_2R_5 + R_4R_5) - \theta_1\theta_2(R_2R_3 + R_2R_5 + R_3R_5)\Big] \\
&+ \theta_1\theta_2 C^{*2}(R_2R_4 + R_2R_5 + R_4R_5) \\
&+ I^*\Big\{\theta_2 S^*\Big[\alpha\beta(R_1 + R_2) + \alpha\tau(R_1 + R_5) + \beta\xi\kappa + \xi\kappa\tau\Big] \\
&\qquad - \theta_1\theta_2 C^*[\beta(R_1 + R_5) + \tau(R_1 + R_5)]\Big\} \\
&+ A\kappa \sum_{2\le i<j<k\le 5} R_iR_jR_k + \alpha S^* \sum_{2\le i<j<k\le 5} R_iR_jR_k \\
&- \theta_2 S^*\Big[R_1(R_2R_3 + R_2R_5 + R_3R_5) + R_2(R_4 + R_5) + R_4R_5\Big] \\
&+ C^*\Big\{\theta_1 \sum_{2\le i<j<k\le 5} R_iR_jR_k + \theta_2\Big[R_1(R_2R_4 + R_2R_5 + R_4R_5) + \theta_1\tau(R_1R_3 + R_1R_5 + R_3R_5)\Big] \\
&\qquad + \beta\xi\kappa(R_1 + R_4)\Big\} \\
&+ \sum_{1\le i<j<k<l\le 5} R_iR_jR_kR_l,
\end{aligned}
$$

$$
\begin{aligned}
c_5 = {} & I^{*2}C^*\phi\rho\theta_1\theta_2R_1(\beta + \tau) - \phi\rho\theta_2 I^{*2}S^*R_1(\alpha\beta + \alpha\tau) \\
& + \alpha\phi\rho\theta_2 S^{*2}I^*R_1R_2 + \phi\rho C^*S^*I^*(\theta_1\theta_2R_1R_3 - \alpha\theta_2R_2R_4) \\
& - C^{*2}I^*\phi\rho\theta_1\theta_2R_2R_4 + S^{*2}I^*\phi\rho\theta_1R_1R_2R_4 \\
& - C^*I^*\phi\rho\theta_2R_1R_2R_4 + I^{*2}\phi\rho(\theta_1\tau R_1R_3 + \alpha\beta R_1R_4) \\
& - (I^*S^*\alpha + I^*C^*\theta_1)\phi\rho R_2R_3R_4 + A\kappa\theta_2(C^*R_2R_3R_5 - S^*R_2R_4R_5) \\
& - I^*\phi\rho R_1R_2R_3R_4 + I^*S^*\theta_2\big[(\alpha R_1R_3)(\beta + \tau) + (\beta + \tau)(\xi\kappa R_1)\big] \\
& - \theta_1\theta_2 I^*C^*(\beta + \tau)R_1R_5 - \theta_2 S^{*2}\alpha R_2R_3R_5 \\
& + (\alpha R_4 - \theta_1R_3)\theta_2 S^*C^*R_2R_5 \\
& + (C^{*2}\theta_1\theta_2 + A\kappa R_3 - S^*\theta_2R_1R_3 + C^*R_1)R_2R_4R_5 \\
& - \tau\theta_1 I^*(R_1R_3R_5 + R_1R_4) - \alpha\beta I^*R_1R_4R_5 \\
& - \beta\xi\kappa I^*R_1R_4 + (\alpha S^* + \theta_1C^* + R_1)R_2R_3R_4R_5.
\end{aligned}
$$

According to Matignon's theorem for fractional-order systems [45], when the fractional order satisfies $\alpha \in (0,1)$, the equilibrium point is locally asymptotically stable if the characteristic equation satisfies:

$$
\begin{cases}
a_i > 0, & i = 1, \ldots, 5, \\
|\arg(\lambda)| > \dfrac{\alpha\pi}{2}.
\end{cases}
$$

Due to the complexity of directly verifying the arguments of all roots, we adopt a relaxed criterion from [46]: when $c_1, c_5 > 0$ and no sign conflicts exist among the remaining coefficients, the model stability is dominated by the positivity of the coefficients. Rigorous derivation confirms $c_1, c_5 > 0$; however, since the expressions for the other parameters are overly complex, we employ a numerical approach using a parameter sweep (10^4 combinations of parameter sets).

The parameter ranges cover $\theta_1 \in (0.15, 0.25)$ and $\theta_2 \in (0.08, 0.12)$, utilizing Latin hypercube sampling (LHS) with $n = 10^4$. As illustrated in Figure A1, c_2, c_3, c_4, c_5 remain strictly positive across all combinations. Referring to Figure 3 in Section 6.1, the model converges to the positive equilibrium point under the typical parameters $\theta = 0.25$ and $\delta = 0.12$.

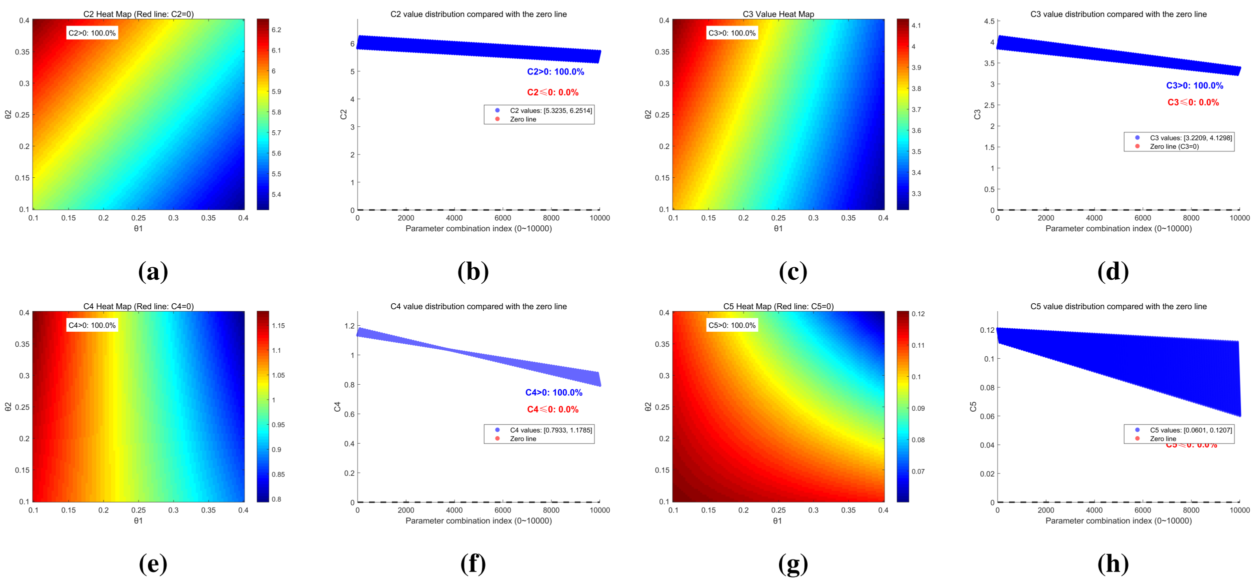

Figure A1. Validation results of coefficients c_2, c_3, c_4, c_5.

Based on the comprehensive stability analysis of c_2, c_3, c_4, c_5, all Hurwitz criteria remain strictly greater than zero within the parameter range $\theta_1, \theta_2 \in [0.1, 0.4]$. The distribution plots exhibit excellent continuity; specifically, c_2 and c_3 show significant sensitivity to variations in both parameters, c_4 is more sensitive to θ_2, while c_5 maintains a relatively stable positive distribution throughout the parameter domain. Crucially, even under the most unfavorable parameter combinations, the minimum values of each criterion remain far from the zero boundary, providing a sufficient safety margin for system stability. In conclusion, when $c_2, c_3, c_4, c_5 > 0$ are simultaneously satisfied, the model is confirmed to be locally asymptotically stable at the positive equilibrium point.

References

1. Z. Sha, S. Zhu, D. Jian, D Xiong, Overcoming language barriers via machine translation with sparse Mixture-of-Experts fusion of large language models, *Inf. Process. Manag.*, **62** (2025), 104078. https://doi.org/10.1016/j.ipm.2025.104078

2. K. Shu, A. Sliva, S. Wang, J. Tang, H. Liu, Fake news detection on social media: A data mining perspective, *ACM SIGKDD Explor. Newsl.*, **19** (2017), 22–36. https://doi.org/10.1145/3137597.3137600

3. S. Vosoughi, D. Roy, S. Aral, The spread of true and false news online, *Science*, **359** (2018), 1146–1151. https://doi.org/10.1126/science.aap9559

4. D. J. Daley, D. G. Kendall, Stochastic rumours, *IMA J. Appl. Math.*, **1** (1965), 42–55. https://doi.org/10.1093/imamat/1.1.42

5. D. H. Zanette, Dynamics of rumor propagation on small-world networks, *Phys. Rev. E*, **65** (2002), 041908. https://doi.org/10.1103/PhysRevE.65.041908

6. M. Nekovee, Y. Moreno, G. Bianconi, M. Marsili, Theory of rumour spreading in complex social networks, *Phys. A*, **374** (2007), 457–470. https://doi.org/10.1016/j.physa.2006.07.017

7. D. J. Watts, S. H. Strogatz, Collective dynamics of 'small-world'networks, *Nature*, **393** (1998), 440–442. https://doi.org/10.1038/30918

8. A. L. Barabási, R. Albert, Emergence of scaling in random networks, *Science*, **286** (1999), 509–512. https://doi.org/10.1126/science.286.5439.509

9. X. Chen, N. Wang, Rumor spreading model considering rumor credibility, correlation and crowd classification based on personality, *Sci. Rep.*, **10** (2020), 5887. https://doi.org/10.1038/s41598-020-62585-9

10. M. Kivelä, A. Arenas, M. Barthelemy, J. P. Gleeson , Y. Moreno , M. A. Porter, Multilayer networks, *J. Complex Netw.*, **2** (2014), 203–271. https://doi.org/10.1093/comnet/cnu016

11. N. Hamdan, A. Kilicman, A fractional order SIR epidemic model for dengue transmission, *Chaos Solitons Fractals*, **114** (2018), 55–62. https://doi.org/10.1016/j.chaos.2018.06.031

12. A. A. Kilbas, H. M. Srivastava, J. J. Trujillo, *North-Holland Mathematics Studies*, Elsevier, **204** (2006). Available from: https://www.sciencedirect.com/bookseries/north-holland-mathematics-studies/vol/204/suppl/C.

13. K. Diethelm, *The Analysis of Fractional Differential Equations*, Springer, Berlin, Heidelberg, 2010. https://doi.org/10.1007/978-3-642-14574-2

14. K. Diethelm, N. J. Ford, Analysis of fractional differential equations, *J. Math. Anal. Appl.*, **265** (2002), 229–248. https://doi.org/10.1006/jmaa.2000.7194

15. V. Lakshmikantham, A. S. Vatsala, Basic theory of fractional differential equations, *Nonlinear Anal.*, **69** (2008), 2677–2682. https://doi.org/10.1016/j.na.2007.08.042

16. R. P. Agarwal, M. Benchohra, S. Hamani, A survey on existence results for boundary value problems of nonlinear fractional differential equations and inclusions, *Acta Appl. Math.*, **109** (2010), 973–1033. https://doi.org/10.1007/s10440-008-9356-6

17. H. G. Sun, Y. Zhang, D. Baleanu, W. Chen, Y. Chen, A new collection of real world applications of fractional calculus in science and engineering, *Commun. Nonlinear Sci. Numer. Simul.*, **64** (2018), 213–231. https://doi.org/10.1016/j.cnsns.2018.04.019

18. W. Ding, S. Patnaik, S. Sidhardh, F. Semperlotti, Applications of distributed-order fractional operators: A review, *Entropy*, **23** (2021), 110. https://doi.org/10.3390/e23010110

19. P. Malik, Deepika, Stability analysis of fractional order modelling of social media addiction, *Math. Found. Comput.*, **6** (2023), 670–690. https://doi.org/10.3934/mfc.2022040

20. X. Yue, W. Zhu, The dynamics and control of an ISCRM fractional-order rumor propagation model containing media reports, *AIMS Math.*, **9** (2024), 9721–9745. https://doi.org/10.3934/math.2024476

21. W. Zhu, Dynamic fractional-order ISDR rumor propagation model incorporating refutation mechanism in complex networks, *Sci. Rep.*, **15** (2025), 31137. https://doi.org/10.1038/s41598-025-16369-8

22. S. Dai, L. Zhu, L. He, Y. Dong, Dynamics and control of infectious diseases on complex networks: A theoretical and empirical study, *J. Math. Anal. Appl.*, **557** (2026), 130334. https://doi.org/10.1016/j.jmaa.2025.130334

23. O. P. Agrawal, A general formulation and solution scheme for fractional optimal control problems, *Nonlinear Dyn.*, **38** (2004), 323–337. https://doi.org/10.1007/s11071-004-3764-6

24. D. F. M. Torres, A. B. Malinowska, *Introduction to the Fractional Calculus of Variations,* Imperial College Press, London, 2012. Available from: https://archive.org/details/introductiontofr0000mali.

25. S. A. Rakhshan, S. Effati, Fractional optimal control problems with time-varying delay: A new delay fractional Euler-Lagrange equations, *J. Franklin Inst.*, **357** (2020), 5954–5988. https://doi.org/10.1016/j.jfranklin.2020.03.038

26. C. Dineshkumar, V. Vijayakumar, R. Udhayakumar, K. S. Nisar, A. Shukla, Results on approximate controllability results for fractional stochastic delay differential systems of order $r \in (1, 2)$, *Stoch. Dyn.*, **23** (2023), 2350047. https://doi.org/10.1142/S0219493723500478

27. C. Dineshkumar, Y. Hoon Joo, A note concerning to approximate controllability of Atangana–Baleanu fractional neutral stochastic integro-differential system with infinite delay, *Math. Methods Appl. Sci.*, **46** (2023), 9922–9941. https://doi.org/10.1002/mma.9093

28. H. M. Ali, S. Z. Rida, A. M. Yousef, A. S. Zaki, Dynamical behavior of fractional-order rumor model based on the activity of spreaders, *Prog. Fract. Differ. Appl.*, **9** (2023), 419–428. https://doi.org/10.18576/pfda/090308

29. Y. Li, Y. Liu, J. Zhang, Dynamic analysis of a fractional-order SINPR rumor propagation model with emotional mechanisms, *Fractal Fract.*, **9** (2025), 546. https://doi.org/10.3390/fractalfract9080546

30. L. Huo, L. Wang, X. Zhao, Stability analysis and optimal control of a rumor spreading model with media report, *Phys. A*, **517** (2019), 551–562. https://doi.org/10.1016/j.physa.2018.11.047

31. D. Li, J. Ma, How the government's punishment and individual's sensitivity affect the rumor spreading in online social networks, *Phys. A*, **469** (2017), 284–292. https://doi.org/10.1016/j.physa.2016.11.033

32. Z. Tufekci, Engineering the public: Big data, surveillance, and computational politics, *First Monday*, **19** (2014). https://doi.org/10.5210/fm.v19i7.4901

33. S. P. Sethi, G. L, *Thompson, Optimal Control Theory: Applications to Management Science and Economics*, Springer, Cham, 2000.

34. M. Caputo, Linear models of dissipation whose Q is almost frequency independent–II, *Geophys. J. Int.*, **13** (1967), 529–539. https://doi.org/10.1111/j.1365-246X.1967.tb02303.x

35. I. Podlubny, *Fractional Differential Equations: An Introduction to Fractional Derivatives, Fractional Differential Equations, to Methods of Their Solution and Some of Their Applications*, Elsevier, 1998.

36. H. L. Li, L. Zhang, C. Hu, Y. L. Jiang, Z. Teng, Dynamical analysis of a fractional-order predator-prey model incorporating a prey refuge, *J. Appl. Math. Comput.*, **54** (2017), 435–449. https://doi.org/10.1007/s12190-016-1017-8

37. A. M. Lyapunov, The general problem of the stability of motion, *Int. J. Control*, **55** (1992), 531–534. https://doi.org/10.1080/00207179208934253

38. E. X. DeJesus, C. Kaufman, Routh-Hurwitz criterion in the examination of eigenvalues of a system of nonlinear ordinary differential equations, *Phys. Rev. A*, **35** (1987), 5288–5290. https://doi.org/10.1103/PhysRevA.35.5288

39. R. M. Anderson, R. M. May, *Infectious Diseases of Humans: Dynamics and Control*, Oxford University Press, 1991. https://doi.org/10.1093/oso/9780198545996.001.0001

40. Y. Ding, Z. Wang, H. Ye, Optimal control of a fractional-order HIV-immune system with memory, *IEEE Trans. Control Syst. Technol.*, **20** (2012), 763–769. https://doi.org/10.1109/TCST.2011.2153203

41. J. P. LaSalle, The Stability of Dynamical Systems, *CBMS-NSF Regional Conference Series in Applied Mathematics*, SIAM, 1976. https://doi.org/10.1137/1.9781611970432

42. Y. Li, Y. Q. Chen, I. Podlubny, Stability of fractional-order nonlinear dynamic systems: Lyapunov direct method and generalized Mittag–Leffler stability, *Comput. Math. Appl.*, **59** (2010), 1810–1821. https://doi.org/10.1016/j.camwa.2009.08.019

43. L. S. Pontryagin, V. G. Boltyanskii, R. V. Gamkrelidze, E. F. Mishchenko, *The Mathematical Theory of Optimal Processes*, John Wiley and Sons, New York, 1962. Available from: https://archive.org/details/mathematicaltheo0000pont.

44. Z. Yue, L. Wang, Lurkers, propagator classification and clarifiers in rumor propagation: A study of dynamics analysis and optimal control strategies, *Int. J. Dyn. Control*, **13** (2025), 363. https://doi.org/10.1007/s40435-025-01877-2

45. D. Matignon, Stability results for fractional differential equations with applications to control processing, in *Computational Engineering in Systems Applications*, **2** (1996), 963–968. Available from: https://www.researchgate.net/publication/2581881.

46. M. S. Tavazoei, A note on fractional-order derivatives of periodic functions, *Automatica*, **46** (2010), 945–948. https://doi.org/10.1016/j.automatica.2010.02.023